Published in final edited form as:
Inorg Chem. 2003 September 8; 42(18): 5722–5734.

Five- to Six-Coordination in (Nitrosyl)iron(II) Porphyrinates: Effects of Binding the Sixth Ligand.

Graeme R. A. Wyllie[†], **Charles E. Schulz**[*,‡], and **W. Robert Scheidt**[*,†]

† *University of Notre Dame*

‡ *Knox College*

Abstract

We report structural and spectroscopic data for a series of six-coordinate (nitrosyl)iron(II) porphyrinates. The structures of three tetraphenylporphyrin complexes [Fe(TPP)-(NO)(L)], where L = 4-dimethylaminopyridine, 1-methylimidazole and 4-methylpiperidine, are reported here to a high degree of precision and allow observation of several previously unobserved structural features. The tight range of bonding parameters for the {FeNO} moiety for these three complexes suggests a canonical representation for six-coordinate systems (Fe–N_p = 2.007 Å, Fe–N(NO) = 1.753 Å, ∠FeNO = 138.5°). Comparison of this data with that obtained previously for five-coordinate systems allows the precise determination of the structural effects of binding a sixth ligand. These include lengthening of the Fe–N(NO) bond and a decrease in the Fe–N–O angle. Several other aspects of the geometry of these systems are also discussed including the first examples of off-axis tilting of a nitrosyl ligand in a six-coordinate $\{FeNO\}^7$ heme system. We also report the first examples of Mössbauer studies for these complexes. Measurements have been made in several applied magnetic fields as well as in zero field. The spectra differ from their five-coordinate analogues. In order to obtain reasonable fits to applied magnetic field data, rotation of the electrical field gradient is required, consistent with differing *g*-tensor orientations in the five- vs. six-coordinate species.

Introduction

The interaction of nitric oxide(NO) with heme is of tremendous physiological importance and is vital to a number of biological processes including neurotransmission, vasodilation and blood clotting.[1] Although the absolute physiological importance of this ligand was not recognized until the 1980s, studies of NO binding to synthetic iron porphyrins date back to the early 1970s.[2,3] However, since NO was recognized as Science's "Molecule of the Year" in 1992,[4] there has been a dramatic upsurge in the amount of research in this field. Indeed, the last few years have seen the publication of not only a journal dedicated purely to this diatomic ligand[5] as well as a recent special issue of *Chemical Reviews* which provides comprehensive summaries of several areas of research of this fascinating ligand.[6]

In addition to its major physiological roles, nitric oxide also proves to be an interesting ligand from a chemical standpoint. As a noninnocent ligand, the assignment of oxidation state for NO-coordinated complexes can be complicated. Because this can lead to ambiguous assignment of oxidation states, we adopt the $\{MNO\}^n$ nomenclature of Enemark and Feltham.[7] Here, the metal and nitric oxide is regarded as a discrete unit and "*n*" represents the number of d-electrons of the metal plus the π^* electrons from the nitrosyl. Hence, the iron(II) system is classified as $\{FeNO\}^7$. Interestingly, iron is the only metal for which this $\{MNO\}^7$ state is

*To whom correspondence should be addressed: E-mail Scheidt.1@nd.edu, Fax (574) 631-4044.

Contribution from The Department of Chemistry and Biochemistry, University of Notre Dame, Notre Dame, Indiana 46556 and Department of Physics, Knox College Galesburg, Illinois, 61401

known in porphyrin derivatives. The observed Fe–N–O geometry lies between the linear {MNO}^{6} and more strongly bent {MNO}^{8} systems. The {FeNO}^{7} system also displays several important properties, unique to this system. These include a strong structural trans effect and a Fe–N–O angle of approximately 140°.

This structural trans effect is exhibited in the structures of the two characterized six-coordinate {FeNO}^{7} porphyrinates: [Fe(TPP)(NO)(1-MeIm)][8,9] and [Fe(TPP)(NO)(4-MePip)].[10] This is reflected by a 0.15 – 0.25 Å lengthening of the Fe–N bond trans to the NO. The Fe–N–O unit displays a bent geometry, similar to that observed for other five-coordinate porphyrinate complexes.

Recently, there has been a great deal of interest in the structure of the five-coordinate {FeNO}^{7} system. The early structurally characterized systems of this type were based on tetraaryl porphyrins and invariably displayed some degree of crystallographic disorder of the nitrosyl ligand.[2] A recent paper[11] reported the detailed structures of three octaalkyl substituted systems. In each case, the nitrosyl ligand is ordered and an off-axis tilting of up to 8°; of the Fe–N(NO) bond from the heme normal is observed. In addition, the pair of Fe–N_p bonds in the direction of the nitrosyl ligand tilt are found to be significantly shorter than the opposing pair. A similar off-axis tilt is seen for the five-coordinate {MNO}^{8} system, [Co(OEP)(NO)] although the magnitude of this tilting is substantially less.[12] The off-axis tilt appears to be an intrinsic property of the five-coordinate nitrosyl hemes. This existence of this off-axis tilt is strengthened by two independent DFT simulations of the [Fe(OEP)(NO)] complex,[13,14] both of which recreate the pattern of Fe–N_p bonds and the tilt. The more detailed study[14] rationalizes this tilting in terms of three significant interactions: an σ-antibonding d_{z^2}(metal)–π^*(NO) interaction and two additional π-interactions, d_{z^2}(metal)–π^*(NO) and d_{z^2} (metal)–π(porphyrin) interactions. The presence of a more strongly bent M–N–O moiety as well as the extra electron in the d_{z^2} orbital of the cobalt system also supports the lesser off-axis tilting observed in this case.

In light of these recent advances in the understanding of the geometry of the five-coordinate {FeNO}^{7} complexes, we consider a further examination of the six-coordinate systems both timely and appropriate. Due to its relevance to the biological systems, we concentrate upon systems containing neutral N-donor heterocycles as the sixth ligand. An important issue for the six-coordinate species is whether an off-axis tilt of the Fe–NO group is an intrinsic property of these six-coordinate {FeNO}^{7} nitrosyl hemes. An adequate examination of this issue requires structural data of high accuracy; the original structure reports of the six-coordinate nitrosyls were based on X-ray data collected at room temperature. These data are insufficient for this purpose; the relatively large thermal motion exhibited by the coordinated NO, peripheral groups, ligands and solvent were features that decreased the quality of the structure determinations. We have obtained obtained new X-ray structural data on four six-coordinate derivatives; two are new species and two had been investigated previously. All structural data were collected at 100 K, where the deleterious effects of thermal motion on the structure quality have been substantially diminished. We report the structure of a new six-coordinate complex, [Fe(TPP)(NO)(4-NMe_2Py)] as well as the redetermination of the structures of the species [Fe(TPP)(NO)(1-MeIm)][8] and [Fe(TPP)(NO)(4-MePip)].[10] These structure determinations are substantially enhanced over those reported previously. They provide additional data in understanding the overall bonding picture in these systems. Finally, a fourth structure, that of the picket fence complex [Fe(TpivPP)(NO)(Py)] is reported. Unfortunately, owing to crystallographically imposed symmetry, this structure is not as informative as the previous three.

In addition to the four structures reported here, we also report a series of spectroscopic data for these complexes. UV-vis, IR and EPR spectra are reported and discussed, particularly in

relation to those previously reported for the five-coordinate {FeNO}^{7} systems. In addition we report the Mössbauer spectra for several of these complexes. To our knowledge, these are the first reported examples of Mössbauer spectra for the six-coordinate {FeNO}^{7} porphyrinates. These spectra are discussed both in relation to the five-coordinate systems and in terms of the effect of the sixth ligands.

Experimental Section

General Information

All reactions were carried out using standard Schlenkware techniques unless otherwise noted. 4-Dimethylaminopyridine was recrystallized from toluene prior to use. Pyridine was distilled over CaH_2 prior to use. Tetrahydrofuran was distilled over sodium and benzophenone. Chlorobenzene was stirred with concentrated H_2SO_4, separated, neutralized with $NaHCO_3$ and dried with $MgSO_4$ prior to distillation. This distilled portion was then distilled over P_2O_5 immediately prior to use.[15] This is done to remove free chlorides that may coordinate with the porphyrin. All other solvents and chemicals were used as received (Fisher). Nitric oxide was purchased from Specialty Gases and purified by passing through a trap containing 4 Å molecular sieves immersed in an ethanol/dry ice slurry. This is done to remove higher oxides of nitrogen.[16] Synthesis of [H_2(TPP)] was carried out using the method of Adler et al.[17] [Fe(TPP)(Cl)] was prepared according to the metallation procedure of Adler et al.[18] [H_2(TpivPP)] was prepared according to a local modification of the reported synthesis.[19] This was metallated by stirring 150 mg of the free base overnight with 100 mg of $FeCl_2$ in 25 mL of THF and 0.2 mL of 2,6-lutidine.

Solution UV-vis spectra were measured on a Perkin-Elmer Lambda 19 UV/vis/near-IR spectrometer. In most cases, these measurements were done on solutions of the (nitrosyl)iron porphyrin in neat ligand (L). In the case of the 4-NMe_2Py, these measurements were done using a saturated chloroform solution of the ligand as the solvent. IR measurements were done on a Nicolet Nexus 870 FT-IR spectrometer. Samples were prepared by selecting a suitable crystal, gently crushing between two NaCl plates and adding a small amount of Nujol to allow dispersion. In the case of [Fe(TpivPP)(NO)(Py)], the solution IR was measured on the (nitrosyl) picket-fence complex dissolved in neat ligand in a NaCl solution cell. EPR measurements were made on frozen solutions at 77 K on a Bruker EMX EPR spectrometer. In the case of [Fe(TPP)(NO)(4-NMe_2Py)], measurements were made by dissolving [Fe(TPP)(NO)]in a concentrated CH_2Cl_2 solution of 4-NMe_2Py. For the 1-methylimidazole and 4-methylpiperidine complexes, measurements were made by dissolving [Fe(TPP)(NO)] in a 1:1 solution of L:CH_2Cl_2.

Samples were prepared for Mössbauer spectroscopy by weighing approximately 40 mg of selected crystals into a Mössbauer cup. These were then immobilized in place by mixing with a small volume of Apiezon M grease to form a mull. The sample holder was then sealed with epoxy resin to render it airtight. The parameters described in the Discussion section were fit by simultaneous least-squares minimization for spectra taken at multiple fields using a Spin Hamiltonian model which takes into account spin fluctuation effects[20] induced by spin-spin interactions, following the approach of Hoy et al.[21] The *g*-values used in these fits were constrained to those obtained from the experimental EPR spectra.

Synthesis of [Fe(TPP)(NO)(L)]

[Fe(TPP)(NO)] was prepared using a modification of the previously reported synthesis.[2] 200 mg of [Fe(TPP)(Cl)] was weighed into a Schlenk flask and 5 mL of chloroform, 0.5 mL of methanol and 0.1 mL of pyridine were added. The solution was purged with argon followed by bubbling of nitric oxide for approximately 5 minutes. 50 mL of methanol was added and the solution stirred to ensure mixing. This resulted in the precipitation of [Fe(TPP)(NO)] which

was isolated by filtration onto sintered glass. 100 mg of this solid was then dissolved in 5 mL of chloroform. 1 mL of this was placed in a 5 mL beaker along with 2 mL of the ligand and 0.5 mL of methanol. In the case of 4-NMe_2Py, a saturated solution of the ligand in chloroform was prepared and 2 mL of this was used. The beaker was placed in a crystallization jar equipped with a rubber stopper and 0.5 mL of 1-propanol, 3 mL of the ligand and 2 mL of chloroform were added outside the beaker. The system was purged with argon then nitric oxide was bubbled through the outer and inner solutions for approximately 5 minutes each. The jar was then sealed and crystals were found to grow after 1 week. In some cases, the five-coordinate species is also found to crystallize, but it was possible to discern the two species upon the basis of crystal morphology. In general, the six-coordinate crystals possess an irregular morphology. This contrasts with the five-coordinate system which forms regular tetragonal bipyramidal crystals. UV-vis (4-NMe_2Py:CH_2Cl_2, 1:4) 416, 554, 586 nm; (1-MeIm:CH_2Cl_2, 1:4) 416, 543, 583, 641 nm; (4-MePip:CH_2Cl_2, 1:4) 417, 463, 554, 591 nm.

Synthesis of [Fe(TpivPP)(NO)(py)]

This complex was obtained as product from a reaction attempting to form nitronitrosyl derivatives. 120 mg of [Fe(TpivPP)(Cl)] was weighed into a Schlenk flask and 5 mL of chlorobenzene, 0.5 mL of methanol and 0.1 mL of pyridine were added. The solution was degassed and purged with argon for approximately 10 minutes. Nitric oxide was bubbled through the solution via 22 gauge needle for approximately five minutes. The solution color changed from a brownish green to a more reddish brown. After the reaction was complete, the needle was removed and a solution of KNO_2 and 18-Crown-6 in chlorobenzene was added. The solution was stirred before being transferred to 8 mm crystallization tubes. These were layered with hexanes, saturated with NO and sealed. Small crystals were found to form after approximately 2 weeks.

X-ray Structure Determinations

Crystalline samples were placed in inert oil, mounted on a glass fiber attached to a brass mounting pin, and transferred to the cold gas stream of the diffractometer. Crystal data were collected and integrated using a Bruker Apex system, with graphite–monochromated Mo Kα (λ = 0.71073 Å) radiation. Data collections were carried out at 100 K for all complexes. All structures were solved using the direct methods program SHELXS.[22] All nonsolvent heavy atoms were located using subsequent difference Fourier syntheses. The structures were refined against F^2 with the program SHELXL.[23] in which all data collected were used including negative intensities. All nonsolvent heavy atoms were refined anisotropically. All nonsolvent hydrogen atoms were idealized using the standard SHELXL idealization methods. Complete crystallographic details are given in the Supporting Information and are summarized in Table 1. [Fe(TPP)(NO)(1-MeIm)]·$CHCl_3$ was found to possess a disordered nitrosyl with the oxygen atom disordered over two possible positions. These were refined and found to have relative occupancies 85% for the major position and 15% for the minor. The major position is denoted O1A in the crystallographic tables and the minor position as O1B. [Fe(TPP)(NO)(4-MePip)]·$CHCl_3$ is found to contain a disordered chloroform molecule for which 2 distinct orientations can be found. These were refined and found to have relative occupancies 65% and 35%. These were then refined anisotropically and the hydrogen atom idealized for both. [Fe(TpivPP)(NO)(Py)]·C_6H_5Cl has the iron positioned on a 2-fold axis in the space group *C2/c* rendering the molecule 1/2 unique. The complete solvent molecule of the asymmetric unit is located very close to this two fold axis and is transformed into a position in which atoms of both orientations overlap. With the exception of the chlorine atom, this solvent molecule was left isotropic. In addition, the oxygen atom of the nitrosyl ligand is disordered over two positions with equal occupancies.

Results

The crystal structures of four six-coordinate (nitrosyl)iron(II) complexes have been obtained. Two of these, [Fe(TPP)(NO)(4-NMe_2Py)] and [Fe(TpivPP)(NO)(Py)]·C_6H_5Cl are previously unreported. Structures of [Fe(TPP)(NO)(1-MeIm)]·$CHCl_3$ and [Fe(TPP)(NO)(4-MePip)] ·$CHCl_3$ have been previously reported[8,10] from data collected at room temperature. Here we report structures from new crystals with data collected at 100 K.

Table 1 summarizes the crystallographic details for all four structures. Figure 1 shows the ORTEP diagram and partial labelling scheme for [Fe(TPP)(NO)(4-NMe_2Py)]. The side view pictured clearly shows the approximately perpendicular orientation of the nitrosyl and 4-dimethylaminopyridine ligand planes. Figure 2 shows a schematic representation of the porphyrin core showing lateral displacements from the 24-atom mean plane. The iron is shifted out-of-plane in the direction of the nitrosyl ligand and the porphyrin core shows a saddled distortion. ORTEP diagrams for the two other tetraphenylporphyrin systems are shown in Figure 3 ([Fe(TPP)(NO)(1-MeIm)]), which also shows the labelling scheme for the porphyrin core, and Figure 4 ([Fe(TPP)(NO)(4-MePip)]). Core diagrams for these systems are shown in Figures 5 and 6 respectively. The ORTEP and core diagram of [Fe(TpivPP)(NO)(Py)] are shown as Figures S1 and S2 in the Supporting Information. Selected bond lengths and angles for all four new six-coordinate complexes and several related systems are given in Table 2. Overall the Fe–N(NO) bond length is relatively constant. None of the N–O bond lengths are foreshortened because of disorder. All systems contain a bent Fe–N–O group with the angle ranging from 137.0 to 139.8°. In all cases, the iron is displaced from the 24-atom mean plane in the direction of the nitrosyl ligand. These displacements are generally smaller than those observed for five-coordinate systems.

The dihedral angle φ(NO) represents the relative orientation of the nitrosyl ligand with respect to the closest Fe–N_p vector. In all cases, the nitrosyl ligand lies between a pair of Fe–N_p bonds. The corresponding dihedral angle, φ(L) gives the relative orientation of the ligand plane to the closest Fe–N_p vector. The angle (θ) given in Table 2 represents the relative orientation of the nitrosyl ligand with respect to the sixth ligand plane. For all three systems containing a planar ligand, the nitrosyl is found to be approximately perpendicular to this ligand plane. In the case of [Fe(TPP)(NO)(1-MeIm)] which contains two nitrosyl orientations, the major nitrosyl ligand orientation adopts an approximately perpendicular orientation with respect to the 1-methylimidazole ligand plane. The second minor orientation of the nitrosyl is ≈ 45°; from the 1-methylimidazole plane and the angle between the two nitrosyl orientations is 72°.

In both the [Fe(TPP)(NO)(4-NMe_2Py)] and [Fe(TPP)(NO)(1-MeIm)] complexes, the imidazole or pyridine plane is found to be tilted off the heme normal. This is most evident for the 4-NMe_2Py system (Figure 1) where the angle between the porphyrin plane and the ligand plane is approximately 64°. In addition to the overall tilting of the ligand plane, the Fe–N(L) bond is bent away from the heme normal by 3.3°; for 1-MeIm and 6.3°; for 4-NMe_2Py. Such tilting of imidazole and pyridine based ligands has been observed previously for a number of systems.[24]

The nitrosyl stretching frequencies for all systems are also given in Table 2. In all cases, these values are lower than that observed for the five-coordinate systems. This is consistent with those results previously obtained. EPR data was also obtained for several systems and this data is summarized in Table 4. All complexes displayed rhombic EPR spectra consistent with that expected for a six-coordinate nitrosyl complex. The EPR spectrum of the frozen solution of [Fe(TPP)(NO)(1-MeIm)] shows a clearly visible nine-line hyperfine splitting pattern which is well-resolved on the g_{mid} resonance.

Mössbauer spectra were collected at 4.2 K in zero field for [Fe(TPP)(NO)(1-MeIm)] and [Fe (TPP)(NO)(4-MePip)]. Spectra were also collected in applied magnetic fields at 4.2 K and over a range of temperatures in zero field. Mössbauer spectroscopic data for these systems and related complexes will be discussed subsequently. The parameters described in the Discussion were fit by least-squares minimization, with the *g*-values constrained to those obtained from the experimental EPR spectra.

Discussion

Synthetic Aspects

The isolation of a pure six-coordinate $\{FeNO\}^7$ porphyrinate is synthetically challenging. A recent review[25] collected all known structures of porphyrinate complexes containing a coordinated nitrosyl ligand. For the $\{FeNO\}^7$ system, the complexes reported are dominated by the five-coordinate state. Given the sheer number of ligands that have been reported coordinating to heme, one would expect many more six-coordinate model complexes to have been reported, especially considering its biological relevance. Yet there are only three: [Fe (TPP)(NO)(1-MeIm)],[8] [Fe(TPP)(NO)(4-MePip)][10] and [Fe(TpivPP)(NO)(NO_2)]–.[26,27] The small number of structures reflects the difficulty of actually isolating pure samples of such complexes.

It is clear that the coordinated nitrosyl ligand discourages the coordination of a sixth ligand in $\{FeNO\}^7$ hemes. Sharma and Traylor,[28] in contrasting the binding constants for NO and CO systems, noted that the binding constant for an imidazole ligand decreases by over three orders of magnitude when NO is coordinated in an $\{FeNO\}^7$ heme. Although there have been extensive spectroscopic measurements made on six-coordinate systems, the majority of such work is based on solution measurements where a large excess of the sixth ligand can overcome the reduced binding constant. However, in attempting to obtain an isolated solid sample of these complexes, addition of larger quantities of the desired ligands does not solve this problem.

In carrying out our investigation of this system, we attempted the synthesis of several new six-coordinate $\{FeNO\}^7$ complexes using a series of alkyl-substituted imidazole, pyridine, and piperidine ligands and a number of different porphyrins.[29] These synthetic efforts generally proved unsuccessful. Several attempted syntheses yielded powders that were characterized by IR-spectroscopy as either mixtures of the five- and six-coordinate complexes or more usually the five-coordinate complex. Simply increasing the concentration of the desired coordinating ligand had little effect upon this. It appears that the only reliable method for obtaining bulk solid samples of the six-coordinate complexes is by growing single crystals. However, a great many of the attempted systems either failed to yield any crystals or the ubiquitous five-coordinate complexes were found to crystallize.

One new six-coordinate $\{FeNO\}^7$ complex was obtained with 4-Dimethylaminopyridine as the sixth ligand. 4-NMe_2Py is a solid at room temperature. Hence, a concentrated solution of the 4-NMe_2Py in chloroform was used instead of the neat ligand.[30] Crystals were identified by IR spectroscopy and the six-coordinate complex was confirmed by X-ray crystallography. The structure is shown in Figure 1. We were also able to reprepare crystalline [Fe(TPP)(NO) (1-MeIm)][8] and [Fe(TPP)(NO)(4-MePip)].[10] The structures of these complexes are shown in Figures 3 and 4 respectively.

It is worth noting that the three successfully used sixth ligands (4-NMe_2Py, 4-MePip and 1-MeIm) are all strongly basic. This is in accord with the studies of Choi and Ryan[31] who noted that ligand pK_a and binding constant to [Fe(Por)(NO)] are strongly correlated. 4-Dimethylaminopyridine and [Fe(TPP)(NO)] had the highest $K_{NO–L}$, which at 8.8 is still very small. The difference in ligand binding constants for different ligand systems is supported by

an earlier series of observations by Maxwell and Caughey.[32] They found that addition of 1-methylimidazole to a solution of (nitrosyl)protoporphyrin IX complex results in a mixture of five- and six-coordinate complexes, as determined by IR spectroscopy. The corresponding system with pyridine as the ligand contains a proportionally higher concentration of the five-coordinate complex. Ligand binding constants were also reported for the iron protoporphyrin-IX dimethyl ester system.[31] In all cases, K_{NO-L} was found to be smaller for this octaalkyl system relative to the tetraphenylporphyrin system. Thus a six-coordinate OEP complex would also be expected to have small ligand binding constants. In addition, the six-coordinate OEP complexes appear to be more soluble than the TPP complexes, particularly in solutions of neat ligand. A combination of these factors explains why at the time of writing no six-coordinate {FeNO}^{7} complex containing OEP has been isolated or structurally characterized.

Molecular Structures

We report here the molecular structures of four six-coordinate {FeNO}^{7} complexes, three at high precision. There are several structural features shared by the three TPP complexes. In all cases, the nitrosyl ligand is bent with an Fe–N–O angle of ~140°, which lies between the linear {MNO}^{6} and strongly bent (≈120°) {MNO}^{8} systems and is characteristic of the intermediate {FeNO}^{7} state. The projection of the nitrosyl ligand onto the porphyrin plane is orientated about midway between a pair of Fe–N_p bonds. The iron atom is displaced from the mean 24-atom porphyrin plane by 0.04–0.06 Å in the direction of the nitrosyl. In all three cases, the porphyrin core has significant deviations from planarity. The distortions are best described as a D_{2d} saddling of the core, rather than the more common D_{2d} ruffing of the core. (See Figures 2, 5, and 6). This saddling is most extreme in the case of the 1-MeIm complex (Figure 5). We note that the saddling of the porphyrin core is an unusual core distortion for a low-spin iron (II) porphyrinate. However, we see no obvious reason for this feature to be common to all three TPP derivatives.

For [Fe(TPP)(NO)(4-NMe_2Py)], one of the more noticeable features is the tilting of the axial pyridine ligand plane from the normal to the heme plane (Figure 1). The dihedral angle between the 24-atom porphyrin plane and the pyridine plane is 65.2°. A similar distortion is observed for the [Fe(TPP)(NO)(1-MeIm)] system although the magnitude of the tilting is less (dihedral angle between the two planes is 81.6°). The 4-MePip complex, on the other hand, contains a nonplanar sixth ligand. However, in all three systems, the Fe–N(L) bond is tilted off-axis (i.e, tilted with respect to the heme normal).

The 4-NMe_2Py and 4-MePip complexes possess a completely ordered nitrosyl ligand, whereas the 1-MeIm complex has the NO ligand disordered over two positions but with one major orientation. [Fe(TpivPP)(NO)(Py)] also has the NO ligand disordered over two positions resulting from the required crystallographic twofold symmetry. This feature, as well as the presence of the bulky picket (pivalamido) groups, leads to a structure that is of lower precision. The twofold symmetry also obscures any possible off-axis tilts of either axial ligand. Nonetheless, the structural features are similar to those of the tetraphenylporphyrin systems.

Selected bond lengths and angles for all six-coordinate {FeNO}^{7} complexes are reported in Table 2. Values are given for both the current low-temperature structure determinations as well as the previously reported room-temperature structure determinations. We first observe that the coordination group parameters, except for the Fe–N(L) distance trans to NO, are very similar over the entire set of [Fe(Por)(NO)(L)] (L = neutral nitrogen donor) complexes. In particular, the geometry of the {FeNO}^{7} moiety appears to independent of the identity of the sixth (trans) ligand. Averaged values for the three low-temperature structure determinations, which have an especially tight range of values for the {FeNO}^{7} coordination group, are given as entry 4 of Table 2 and labelled as <[Fe(Por)(NO)(L)]>. We believe this represents a “canonical” or best value of the FeNO geometry in the six-coordinate {FeNO}^{7} system.

The complex [Fe(TPP)(NO)(4-MePip)] was originally obtained both as chloroform solvate and an unsolvated form[10] while only a solvated form of [Fe(TPP)(NO)(1-MeIm)] is known.[8] Differences between the earlier structural determinations and <[Fe(Por)(NO)(L)]> include slightly smaller iron atom displacements, slightly longer Fe–N(NO) and N–O bond lengths at the lower temperature. Additionally, the disordered chloroform solvate is much better defined at the lower temperature. These small differences between the low-temperature and room-temperature structure determination are consistent with larger thermal motion naturally found at the higher temperature.

Further differences are found between the low- and room-temperature structures of the 1-MeIm derivative. The axial Fe–N(Im) bond lengths are comparable as is the relative orientation of the imidazole. The relative orientations of the NO ligands are significantly different at the two temperatures with two distinct orientations of the NO ligand at each temperature. At low temperature, the relative population of the major NO orientation, O1A, increases to 85% (from 67%). The projection of the nitrosyl is midway between a pair of $Fe–N_p$ bonds, similar to that observed for both five-coordinate and other six-coordinate $\{FeNO\}^7$ porphyrinate complexes. This low-temperature orientation change leads to an increase in the dihedral angle between the nitrosyl and imidazole ligand planes that approaches orthogonality, a characteristic of other six-coordinate nitrosyl systems. Axial ligand orientations for both temperatures are shown on the core diagrams in Figure 5.

The significant differences in the nitrosyl ligand orientations in [Fe(TPP)(NO)(1-MeIm)] can be rationalized in terms of solid-state dynamic motion of the NO. Solid-state dynamic disorder in the five-coordinate cobalt system, [Co(TPP)(NO)], has been reported.[33] At higher temperature, NO is able to freely rotate about the M–N(NO) axis but becomes locked into a stable low-energy orientation as the temperature decreases. Similar ligand behavior therefore seems plausible for the isomorphous iron systems. Theoretical calculations, originally by Hoffmann,[34] for nonporphyrinic systems and later by Parrinello et al.[35] and Patchkovskii and Ziegler[36] expressly for the iron porphyrinate system, calculate a very low-energy barrier to NO rotation about the Fe–N(NO) bond. The lowest energy state determined from the DFT calculations[35] is that where the nitrosyl lies approximately between a pair of $Fe–N_p$ vectors which corresponds with the major orientation observed at low-temperature.

We discuss the relative geometries of the {FeNO} unit in the five- and six-coordinate $\{FeNO\}^7$ species below. However, before comparing these two coordination numbers, we first examine the structural trans effect exerted by the nitrosyl ligand. This characteristic lengthening of the Fe–N(L) bond trans to the NO had been noted for the previous [Fe(TPP)(NO)(L)] structures.[8,10] For the three low-temperature TPP structures, the Fe–N(L) length ranges from 2.173 Å for [Fe(TPP)(NO)(1-MeIm)] to 2.285 Å for [Fe(TPP)(NO)(4-MePip)]. Estimates of the magnitude of this increase in Fe–N(L) can be determined by comparison with a series of bis-ligated six-coordinate iron(II) porphyrin complexes containing a variety of N-bonded ligands.[37–39] Bis-imidazole complexes[37] display axial Fe–N(L) bonds ranging from 2.004(2) Å[37a] to 2.017(4) Å[37c] compared to 2.173(2) Å in [Fe(TPP)(NO)(1-MeIm)], a lengthening of ~0.16 Å. The Fe–N(L) bond in $[Fe(Por)(L)_2]$, where L is either pyridine or a substituted pyridine varies from 1.996(2) Å[38c] to 2.039(1), Å[38b] with a median value of 2.019 Å. This gives a lengthening of ~0.22 Å for the Fe–N(L) bond in $[Fe(TPP)(NO)(4\text{-}NMe_2Py)]$ upon NO coordination, greater than that observed for [Fe(TPP)(NO)(1-MeIm)]. For [Fe(TpivPP)(NO)(Py)], this lengthening is also ~0.22 Å The Fe–N(L) bond length in $[Fe(TPP)(Pip)_2]$ is 2.127(3) Å[39a] and [Fe(TPP)(NO)(4-MePip)] is 2.2851(19) Å, a lengthening of ~0.16 Å. A second unsolvated crystalline polymorph of [Fe(TPP)(NO)(4-MePip)] gives a trans lengthening of ~0.34 Å. We conclude that the magnitude of the structural trans effect appears at least somewhat variable in $\{FeNO\}^7$ heme systems.

The lengthening and weakening of the bond trans to the NO has important physiological repercussions. Breaking of the trans bond upon coordination of nitric oxide is the means by which NO activates the enzyme guanylate cyclase. Coordination of NO to heme leads to the axial iron-histidine bond being broken, subsequent rearrangement of the protein and ultimately activation of the enzyme which is involved in further physiological processes.[40–42] This mechanism is supported by various spectroscopic studies which directly correlate enzyme activation with proximal histidine bond-breaking.[43]

The physiological relevance of the trans effect exerted by NO is also evident in the interaction of NO with hemoglobin. Addition of the allosteric effector inositol hexaphosphate (IHP) to the nitrosylated form of hemoglobin results in exclusive cleavage of the Fe–N(His87) bond of the α-hemes. This results in a tetraheme complex containing two five-coordinate and two six-coordinate (nitrosyl)hemes. This is supported by EPR analysis where the spectrum exhibits features characteristic of both coordination numbers[44] and also by IR spectroscopy.[32] Nitric oxide coordinates preferentially to the α-hemes and addition of a stoichiometric amount of NO results in the partially nitrosylated $\alpha^{NO}\beta^{deoxy}$ complex. Hemoglobin is known to possess two distinct states, the T (tense) low ligand-affinity structure and the R (relaxed) high ligand-affinity structure. Yonetani et al.[49] have shown that transition between the two states can be linked to the reversible cleavage of the Fe–N(His) bond in the α-heme. The coordination number is found to be sensitive both to the presence of IHP[32] and the pH of the environment. The coordination number of the α-heme can be correlated with state based upon UVRR examination of the Trp and Tyr residues at the $\alpha 1$-$\beta 2$ subunit interface. Further work by Yonetani et al.[50] showed that the behavior of the residues at the interface is not synchronous although there is a direct relationship between the cleaving of the Fe–N(His) residue in the α-heme and the T-like character of Trp-β437.

Off-axis Fe–N(NO) Tilt

Several high quality structures of five-coordinate {FeNO}^{7} complexes have been recently determined[11] and reveal an unexpected distortion of the N_4FeNO coordination geometry that hitherto had been concealed by nitrosyl disorder. For all ordered nitrosyl complexes, the nitrosyl ligand is tilted off-axis: the Fe–N(NO) bond is tilted from the heme normal in the direction of the nitrosyl oxygen. This tilt angle ranges from 6.5°; to 8.2°. In addition to the ligand tilting, there is also an asymmetric interaction between the iron and the pyrrolic nitrogens of the porphyrin ring. This is manifested in long and short pairs of Fe–N_p bonds, with the short pair bracketing the NO tilt direction and projection of the NO onto the porphyrin plane. A similar pattern, although of lesser magnitude is observed for the {MNO}^{8} complex [Co(OEP)(NO)].[12] Several model calculations of the [Fe(Por)(NO)] complex[13,14,35,36] have reproduced both the pattern of the Fe–N_p bonds and the tilting of the ligand; the work of Ghosh and Wondimagegn[14] also rationalizes the differing degrees of tilting between the iron and cobalt systems.

The off-axis tilting of the nitrosyl ligand has thus been clearly shown to occur for five-coordinate complexes. But is such a distortion also observed for the six-coordinate {FeNO}^{7} complexes? The previously reported structures had not been of sufficient precision to allow such a determination to be made. In light of the new structural data, we are now able to address the issue of tilting in the six-coordinate systems. Fe–N(NO) tilt angles for both the five- and six-coordinate systems are given in Table 3. A tilting of the Fe-N(NO) bond is seen in the six-coordinate complexes, but the extent of the tilting is smaller (1.8°; – 6.5°). However, the pattern of long and short Fe–N_p bonds concomitant with NO tilting is clearly observed in [Fe(TPP)(NO)(1-MeIm)] and [Fe(TPP)(NO)(4-NMe_2Py)]; it is more ambiguous in the [Fe(TPP)(NO)(4-MePip)] case. Individual values of Fe–N_p bond distances are given in Table 3. In the table, the Fe–N_p bonds expected to be the short pairs (those bracketing the NO ligand projection) are

italicized whilst those expected to be the long pairs are given in bold. For both the 1-MeIm and 4-NMe_2Py systems, the difference between the long and short pairs of bonds (Δ(Fe–N_p)) is comparable to that observed for the various five-coordinate complexes. We conclude that the ligand titling and asymmetric interaction of iron with the pyrrole nitrogen atoms is present in the six-coordinate {FeNO}^{7} species as well as in the five-coordinate species.

Comparison of Five- and Six-coordinate Species

The recent high-precision structures[11] of several [Fe(Por)(NO)] species also allow the definition of a representative or "canonical" value for five-coordinate {FeNO}^{7} geometry. This canonical value, along with values for individual species, is given in Table 2. We believe that the two canonical values represent a true and meaningful picture of the FeNO geometry for both coordination numbers and allow us to make accurate, quantitative comparisons.

An increase in the coordination number would be expected to affect the bonding between the iron and the ligands in the coordination group. Nonetheless, certain bonding parameters are unaffected by the presence of the additional ligand. The nitrosyl ligand maintains an orientation roughly midway between a pair of Fe–N_p bonds. The average Fe–N_p bond length remains essentially constant at 2.008 to 2.009 Å upon coordination of the sixth ligand. Any change in the length of the N–O bond of the nitrosyl is also minimal (0.006 Å) and below the significance of the determinations. As noted earlier, a similar pattern of NO tilts and asymmetry in the equatorial Fe–N_p bonds appears to be present for both coordination numbers.

However, there are significant differences between the bonding geometry of the five- and six-coordinate complexes, the first of which is the modest lengthening (~0.025 Å) of the Fe–N (NO) bond for the six-coordinate complexes. The Fe–N–O angle decreases by approximately 5°; for the six-coordinate systems. Both features are consistent with a modest decrease in Fe–N(NO) σ and π-bonding and a weakened Fe–N(NO) bond. As mentioned above, there is little variation in the FeNO geometry for the various six-coordinate complexes. We conclude that it is simply the presence of the sixth ligand rather than its identity that causes this change in bonding. This is not the case spectroscopically where both the presence and identity of the sixth ligand affect the various spectroscopic parameters. These include both the ν(NO) stretching frequency in the infrared spectra and the various parameters of the Mössbauer spectra. This is discussed in more detail later. The decrease in the Fe–N–O angle can be justified in terms of the N-donor ligand providing additional electron density at the iron center. We suggest that this increases the antibonding component of the interaction between the iron and the NO and the Fe–N–O is further distorted from linearity to minimize this interaction. A similar explanation[34] has been used to rationalize the greater bending of the nitrosyl observed for five-coordinate {CoNO}^{8} complexes. In addition, the greater bending of the FeNO moiety is supported by an optimized model of the six-coordinate [Fe(Por)(NO)(Im)] complex by Parrinello et al.[35] where an Fe–N–O angle of 138°; is calculated. Another significant difference between the two coordination states is the position of the iron atom relative to the plane of the porphyrin. In the six-coordinate system, the iron moves approximately 0.20 Å into the plane. Figure 7 shows schematic representations of the coordination environment for the iron for both the five- and six-coordinate {FeNO}^{7} systems.

Nitrosyl stretching frequencies ν(NO) in the six-coordinate complexes decrease relative to the five-coordinate systems (Table 2). For multiply-bonded, diatomic ligands such as NO, a decreased ν(NO) is typically associated with an increased population of the π^*(N–O) orbitals. This bonding picture is derived from the related, well-known carbonyl systems where an increased π^* population is associated with an enhanced M→C π-bond.[45] Strengthening the M–CO bond occurs at the cost of weakening the C–O bond; plots of ν(M–C) vs. ν(C–O) have negative slopes or negative correlations.[46] This negative correlation holds for carbonyl heme complexes, although different correlations (slopes) of ν(CO) against ν(Fe–CO) are observed

for the five-vs. six-coordinate systems.[47] Thus, the slope of the line for five-coordinate carbonyl hemes is −0.37 but is −0.73 for six-coordinate derivatives. Spiro et al.[47] have shown that this negative correlation also holds for a series of 5-coordinate {FeNO}^{7} porphyrinate complexes. Further, Spiro et al. have suggested that the same correlation should apply equally well to six-coordinate {FeNO}^{7} porphyrinate complexes.

However, as described in this study, the Fe–N(NO) interaction appears to be weakened on coordination of the sixth ligand, as evinced by the lengthening of this bond. This apparent decrease in Fe–N(NO) bond strength should lead to an expected decrease in ν(Fe–NO), relative to the five-coordinate species, that is also accompanied by the observed decrease in ν(NO). This is inconsistent with the suggested[47] identical negative correlation of ν(NO) with ν(Fe–NO) for both the five- and six-coordinate derivatives. Rather, we suggest that the five- and six-coordinate nitrosyl derivatives should have distinctive correlations of ν(NO) with ν(Fe–NO) similar to that seen for the carbonyls. Interestingly, DFT calculations by Spiro et al. even predicted a positive correlation for the coordination of a sixth ligand trans to NO. Unfortunately, due to experimental difficulties, the spectroscopic measurements needed to complete the correlation for six-coordinate complexes have not yet been made.[48]

EPR Spectra

The EPR spectrum of [Fe(TPP)(NO)(1-MeIm)] obtained at 77 K clearly shows a 9-line hyperfine splitting pattern arising from the interaction of the unpaired electron with both the nitrosyl and sixth ligand nitrogen atoms. Similar spectra are observed for both the 4-NMe_2Py and 4-MePip complexes. The *g*-values and hyperfine splitting constants for several six-coordinate and the five-coordinate [Fe(TPP)(NO)][3] and [Fe(OEP)(NO)] complexes[51] are given in Table 4. Overall, the *g*-values and hyperfine splitting constants obtained for these six-coordinate {FeNO}^{7} systems are consistent with those previously reported.[3,52] The EPR spectra of the five- and six-coordinate species are different, both in the *g*-values and the appearance of the spectra.[53] The well-resolved hyperfine features are also associated with a different *g*-tensor in each complex: g_{min} for the five-coordinate system and g_{mid} for the six-coordinate. A probable explanation for the EPR spectral differences is that the spatial orientation of the *g*-tensor with respect to the molecular framework is different in the two classes of compounds i.e. the orbital for the unpaired electron is different for the two coordination numbers.

EPR measurements carried out on a doped single oriented crystal of [Fe(OEP)(NO)][54] allowed Hayes et al.[51] to determine experimentally the orientation of the *g*-tensor in a five-coordinate heme. These measurements have shown that for the five-coordinate system, g_{min} is very nearly normal to the porphyrin plane, with the unpaired electron occupying an orbital that is primarily d_{z^2} in character. g_{mid} and g_{max} lie within the porphyrin plane albeit not coincident with the Fe–N_p bonds as is usually observed for porphyrin complexes. g_{mid} corresponds approximately to the projection of the N–O bond on the porphyrin plane whereas g_{max} is rotated from this by 90°; and lies between a pair of adjacent Fe–N_p bonds. Thus, the *g*-tensor effectively lies in the porphyrin plane and the normal to the plane. Unfortunately, the lack of a suitable diamagnetic host prevents a similar experimental determination of the *g*-tensor being carried out for a six-coordinate {FeNO}^{7} porphyrinate complexes.

Calculations of Patchkovskii and Ziegler[36] give insight into the possible differences in the *g*-tensor between the two coordination numbers. They have calculated *g*-tensors for both five- and six-coordinate systems. The agreement between the calculated and experimental *g*-tensors for the five-coordinate system are reasonable. However, for the six-coordinate [Fe(Por)(NO)(Im)] system, the calculated g-tensor is markedly different from that of the five-coordinate system. The largest component g_{max} is found to be approximately perpendicular to the FeNO plane. More significantly, g_{min} lies approximately parallel with the N–O bond while g_{mid} is

perpendicular to it. This leads to a completely different *g*-tensor orientation compared to the five-coordinate system with the tensor defined by the nitrosyl ligand and not the iron porphyrinate skeleton as previously observed. This also coincides with the decrease in electron density on the iron calculated by Patchkovskii and Ziegler. Possible experimental verification of the *g*-tensor assignments is provided by the Mössbauer results described below.

Mössbauer Spectra

To our knowledge, Mössbauer spectra have not been previously measured for six-coordinate {FeNO}^{7} porphyrinate derivatives other than an early measurement on nitrosyl hemoglobin.[55,56] The exact molecular state of $Hb(NO)_4$ in this early study is not clear; however, some important conclusions were forthcoming. The unpaired electron occupies a σ-orbital and the large hyperfine interaction implies a strong interaction between NO and iron blurring the distinction between an iron(II) and an iron(III) oxidation state. The investigators noted from the difficulty of obtaining good fits to the experimental Mössbauer data that the problem was a challenging one. With this early study to whet our interest, we undertook to obtain and analyze Mössbauer spectra of six-coordinate {FeNO}^{7} species in zero and applied magnetic field. We hoped that such analyses would enable us to better understand the apparent difference in electronic structure of the five- and six-coordinate nitrosyls.

We have carried out detailed Mössbauer studies on powders derived from crystalline [Fe(TPP)-(NO)(1-MeIm)] and [Fe(TPP)(NO)(4-MePip)] in zero field and in 3, 6, and 8.8 T applied magnetic fields. We were able to prepare adequate bulk samples of these two compounds, but were not able to obtain an adequate bulk sample for [Fe(TPP)(NO)(4-NMe_2Py)]. Additional attempts to study six-coordinate species in frozen solutions utilizing ^{57}Fe-enriched porphyrin samples were unsatisfactory owing to a mixture of species present in the frozen solutions.

Mössbauer results are summarized in Table 5 along with some relevant data for five-coordinate {FeNO}^{7} porphyrinates. The isomer shifts (δ) for [Fe(TPP)(NO)(1-MeIm)] show temperature variation commensurate with a second-order Doppler effect. The values of the isomer shifts are comparable to those previously reported for the five-coordinate [Fe(TPP)(NO)][26] and [Fe (OEP)(NO)][57] complexes. However, these values (~0.35 mm/sec) are smaller than those observed for the related [Fe^{II}(Por)$(L)_2$] systems,[37b,38c] ($\delta \approx 0.45$ mm/s). The isomer shift values are slightly larger than those of the analogous carbonyl complexes (limited number available[19, 58]). Overall, the lower values of isomer shift, relative to most iron(II) porphyrinates, are consistent with the earlier conclusion of Lang et al. that oxidation state distinctions in nitrosylhemoglobin are blurred.

Unlike the isomer shift, the quadrupole splitting (ΔE_q) changes upon coordination of the sixth ligand. There is an expected decrease in ΔE_q as the iron environment changes to the more symmetric (six-coordinate) state. Thus, ΔE_q for the five-coordinate [Fe(TPP)(NO)] species (1.24 mm/s) decreases for both the 1-methylimidazole derivative (0.75 mm/sec) and the 4-methylpiperidine complex (0.91 mm/sec). The lower value for the 1-methylimidazole complex is perhaps the result of the modest π-bonding capability of the imidazole ligand, relative to the σ-only interaction of the 4-methylpiperidine ligand.

In addition to the diagnostic information obtained from the values of the ΔE_q and δ, additional insights into the nature of the six-coordinate {FeNO}^{7} systems can be achieved from an analysis of the spectra obtained in an applied magnetic field. Measurements were carried out at magnetic fields of 3, 6, and 8.8 T to provide for maximal constraints on the fitting parameters. Measurements at zero field were not included in the fits, but the quadrupole splitting and isomer shift were constrained to the values determined using the zero-field spectra.

The spectra were fit using the S = 1/2 spin Hamiltonian

$$H = \mu_B \vec{S} \cdot \tilde{g} \cdot \vec{H} - g_N \mu_N \vec{H} \cdot \vec{I} + \vec{I} \cdot \tilde{Q} \cdot \vec{I} + \vec{S} \cdot \tilde{A} \cdot \vec{I}$$

where $\vec{H}$ is the external applied magnetic field, $\tilde{Q}$ is the quadrupole tensor (which is proportional to the electrical field gradient at the nucleus), and $\tilde{A}$ is the magnetic hyperfine tensor which characterizes the energy of the magnetic interaction between the electron spin $\vec{S}$ and the ^{57}Fe nuclear spin $\vec{I}$. All fits used the experimentally determined EPR *g*-values reported in Table 4 and the measurements made at various magnetic fields. Figure 8 shows the fits obtained for [Fe(TPP)(NO)(1-MeIm)]. In these fits, the electric field gradient (EFG) tensor, the *A*-tensor, and the *g*-tensor were taken to have coincident principal axes. Although the fits obtained mirrored the overall features in the spectra, the quality of the fits were less than optimal.

Accordingly, in an attempt to achieve better fits, the electric field gradient tensor was allowed to rotate[59, 60] with respect to the *A*- and *g*-tensors. When the Euler angles characterizing a rotated EFG are allowed to vary, a better fit to the 1-MeIm spectra is achieved when the EFG *zz*-component is rotated by $\beta = 33°$; towards the *x*-*y* plane of the *g*- and *A*-tensor principal axis system. The overall quality of the fit improved as can be seen from a comparison of Figure 9 with Figure 8 and the results of χ^2 tests. To achieve the best simultaneous fits to spectra taken in applied fields of 3, 6, and 8.8T, we had to abandon our initial assumption that the slow spin fluctuation limit would apply even at the lower fields. Instead fits were made using a dynamic model which includes effects caused by intermediate electron spin fluctuation rates.[20]

Given the off-axis Fe–N(NO) bond, the effective symmetry at the iron site is lower than rhombic, so there is no reason to expect any of the tensor quantities (*g*, *A*, *Q*) to have their principal axes aligned. (See, for example, crystal field calculations on cytochrome P-450 by Champion.[61]) However, the small shifts of the *g*-values from $g = 2$ make the Mössbauer spectra relatively insensitive to the *g*-parameters. The Euler angles thus represent a relative rotation between the *Q*- and *A*-tensors. It has been argued by Patchkovskii and Ziegler[36] that the *g*-tensor component g_{min} must be near the direction of the N–O bond in the six-coordinate complex [Fe(Por)(NO(1-MeIm)] and not along the Fe–N(NO) axis as observed by single crystal EPR for [Fe(OEP)(NO)].[51] While the low symmetry of the iron site precludes simple geometric interpretations of our fit values of the Euler angles, it is also not surprising, given the low symmetry, that Euler angles would be needed to properly characterize the iron environment. While our analysis is not inconsistent with the *g*-tensor component g_{min} being aligned along the N–O axis, the principal axes determined from the Mössbauer fits are not easily related to the molecular coordinates; thus we are unable to absolutely confirm that assignment. Independent confirmation of those theoretical predictions could be made with single-crystal EPR measurements. Further clarification of the relative orientations of the *g*, *A*, and *Q* tensors could also come from the results of ENDOR measurements or molecular structure calculations - valuable avenues for future investigations.

Similar results were obtained for the Mössbauer data obtained for [Fe(TPP)(NO)(4-MePip)], although the quality of the fits are definitely poorer (Table 5 and Supporting Information). The fact that that the rotation angles are somewhat different from those obtained for [Fe(TPP)(NO)(1-MeIm)] may reflect differences in the relative *g*-tensor and EFG orientations because of the differing σ contributions to the d_{z^2} orbital from the two axial ligands.

We have also examined the Mössbauer spectra of the five-coordinate complex [Fe(TPP)-(NO)]. Mössbauer spectra for this compound had been previously reported at zero field and 8 T.[26] We have now measured spectra at several different applied magnetic fields. When all magnetic field data are fit simultaneously, we obtain somewhat different fits from those originally reported (Table 5). This is the result of increasing the amount of information in the fitting process. Importantly however, there is no improvement in the quality of the fits upon

rotation of the EFG tensor. This is consistent with the idea that the *g*-tensor orientations of the five-and six-coordinate species are quite distinct.

Summary

Examples of six-coordinate $\{FeNO\}^7$ porphyrinates utilizing a neutral N-donor as the sixth ligand have been prepared and structurally characterized. Comparison of representative five- and six-coordinate geometries reveal several distinct changes in the {FeNO} moiety as the coordination number is increased (Figure 7). The Fe–N(NO) bond length increases, whilst the FeNO angle decreases as a result in the decrease in Fe→N π-bonding. The characteristic structural trans effect exerted by the nitrosyl in $\{FeNO\}^7$ systems is observed as are structural features that were previously undetectable. Like the five-coordinate system, the nitrosyl ligand exhibits an off-axis tilting of the Fe–N(NO) vector and characteristic short/long pairs of Fe–N_p bonds. We have also collected spectroscopic data on the various six-coordinate complexes. Mössbauer spectra reveal a marked decrease in ΔE_q upon coordination of the sixth ligand and, unlike the five-coordinate systems, require rotation of the electric field gradient to obtain suitable fits. This reflects a *g*-tensor orientation dominated by the orientation of the N–O bond unlike the classical metal-based picture seen for the five-coordinate complex.

Supplementary Material

Refer to Web version on PubMed Central for supplementary material.

Acknowledgements

We thank the National Institutes of Health for support of this research under Grant GM-38401 to WRS. We thank the NSF for EPR support through instrumentation grant NSF-98-70990. We also thank Dr. A. Beatty for assistance with X-ray data collection and Professor R.G. Hayes for helpful discussion on the EPR section.

References and Notes

1. Packer, L., editor. Methods in Enzymology: Nitric Oxide Part B, Physiological and Pathological Processes. 269. Academic Press; San Diego, CA: 1996.
2. Scheidt WR, Frisse ME. J Am Chem Soc 1975;97:17. [PubMed: 1133330]
3. Wayland BB, Olson LW. J Am Chem Soc 1974;96:6037. [PubMed: 4415859]
4. Koshland DE Jr. Science 1992;258:1861. [PubMed: 1470903]
5. Nitric Oxide: Biology and Chemistry. Academic Press; 1997.
6. Richter-Addo, GB.; Legzdins, P.; Burstyn, J., editors. Chem Rev. 102. 2002.
7. (a) Enemark JH, Feltham RD. Coord Chem Rev 1974;13:339.Westcott, BL.; Enemark, JH. Inorganic Electronic Structure and Spectroscopy. In: Lever, ABP.; Solomon, EI., editors. Applications and Case Studies. II. Wiley-Interscience Publications; New York: 1999. p. 403-450.
8. Scheidt WR, Piciulo PL. J Am Chem Soc 1976;98:1913. [PubMed: 1254850]
9. The following abbreviations are used in this paper. Porphyrins: OEP, dianion of octaethylporphyrin; oxoOEC, dianion of oxooctaethylchlorin (2-oxo-3,3′,7,-8,12,13,17,18-octaethylporphyrin); Por, generalized porphyrin dianion; TMP, dianion of meso-tetramesitylporphyrin; TpivPP, dianion of meso-α, α, α, α-tetrakis(o-pival-amidophenyl)porphyrin; TPP, dianion of meso-tetraphenylporphyrin; $TPPBr_4$, dianion of 7,8,17,18-tetrabromo-meso-tetraphenylporphyrin; TTP, dianion of meso-tetratolylporphyrin;. Ligands: 1-MeIm, 1-methylimidazole; 4-MePip, 4-methylpiperidine; $4\text{-}NMe_2Py$, 4-dimethylaminopyridine; 3-CNPy, 3-cyanopyridine; 4-CNPy, 4-cyanopyridine; 4-MePy, 4-methylpyridine; Im, imidazole; 1-VinIm, 1-vinylimidazole; 1-BzIm, 1-benzylimidazole; $1\text{-}BuNH_2$, 1-butylamine; $BzNH_2$, 1-benzylamine; IHP, inositol hexaphosphate; Pip, piperidine; Py, pyridine. Other: EFG, electrical field gradient; N_p, porphyrinato nitrogen. UVRR, ultraviolet resonance Raman.
10. Scheidt WR, Brinegar AC, Ferro EB, Kirner JF. J Am Chem Soc 1977;99:7315.
11. Scheidt WR, Duval HF, Neal TJ, Ellison MK. J Am Chem Soc 2000;122:4651.
12. Ellison MK, Scheidt WR. Inorg Chem 1998;37:382. [PubMed: 11670283]

13. Cheng L, Novozhilova I, Kim C, Kovalevsky A, Bagley KA, Coppens P, Richter-Addo GB. J Am Chem Soc 2000;122:7142.
14. Ghosh A, Wondimagegn T. J Am Chem Soc 2000;122:8101.
15. Armagero, WLF.; Perrin, DD. Purification of Laboratory Chemicals. 4. Butterworth-Heinemann; Woburn, MA: 1997. p. 140
16. Dodd, RE.; Robinson, PL. Experimental Inorganic Chemistry. Elsevier; New York: 1957. p. 253
17. Adler AD, Longo FR, Finarelli JD, Goldmacher J, Assour J, Korsako3 L. J Org Chem 1967;32:476.
18. Adler AD, Longo FR, Kampus F, Kim J. J Inorg Nucl Chem 1970;32:2443.
19. Collman JP, Gagne RR, Halbert TR, Lang G, Robinson WT. J Am Chem Soc 1975;97:1427. [PubMed: 1133392]
20. Schulz CE, Nyman P, Debrunner PG. J Chem Phys 1987;87:5077.
21. Hoy GR, Corson MR, Balko B. Phys Rev B 1983;27:2652.
22. Sheldrick GM. Acta Crystallogr 1990;A46:467.
23. Sheldrick, GM., editor. SHELXL-97. FORTRAN program for crystal structure refinement, ©. Göttingen University; 1997.
24. Freeman HC. Advan Protein Chem 1967;22:257. [PubMed: 4882247]
25. Wyllie GRA, Scheidt WR. Chem Rev 2002;102:1067. [PubMed: 11942787]
26. Nasri H, Ellison MK, Chen S, Hunyh BH, Scheidt WR. J Am Chem Soc 1997;119:6274.
27. Although $[Fe(TpivPP)(NO)(NO_2)]^-$ is nominally classified as a $\{FeNO\}^7$ complex, the properties of this system differ significantly from all other five and six-coordinate $\{FeNO\}^7$ complexes. We describe this complex as a nitronitrosyl system rather than a “pure” nitrosyl and although we list the various data that has been previously reported, in general, these complexes fall outside the scope of interest of this work.
28. Traylor TG, Sharma VS. Biochemistry 1992;31:2847. [PubMed: 1348002]
29. Porphyrin ligands used in these attempts included H_2TMP, $H_2TpivPP$, H_2TTP and H_2OEP as well as H_2TPP.
30. In several other systems where a solution of the ligand was required, problems were encountered with the ligand precipitation. This led to the powder or crystals being coated with the pure ligand. This was not the case with 4-NMe_2Py where no problem with the ligand precipitation was encountered.
31. Choi IK, Ryan MD. Inorg Chim Acta 1988;153:25.
32. Maxwell JC, Caughey WS. Biochemistry 1976;15:388. [PubMed: 1247525]
33. Groombridge CJ, Larkworthy LF, Mason J. Inorg Chem 1993;32:379.
34. Hoffmann R, Chen MML, Elian M, Rossi AR, Mingos DMP. Inorg Chem 1974;13:2666.
35. Rovira C, Kunc K, Hutter J, Ballone P, Parrinello M. J Phys Chem A 1997;101:8914.
36. Patchkovskii S, Ziegler T. Inorg Chem 2000;39:5354. [PubMed: 11154592]
37. Several bis-ligated iron(II) complexes of general formula $[Fe(Por)(L)_2]$ where L in an imidazole derivative have been structurally characterized. The values of Fe–N(L) are as follows: (a) $[Fe(TPP)(1\text{-}MeIm)_2]$, 2.014(5) Å, Hoard, J. L. personal communication to WRS; (b) $[Fe(TPP)(1\text{-}VinIm)_2]$, 2.004(2) Å; $[Fe(TPP)(1\text{-}BzIm)_2]$, 2.017(4), Safo MK, Scheidt WR, Gupta GP. Inorg Chem 1990;29:626.
38. Several bis-ligated iron(II) complexes of general formula $[Fe(Por)(L)_2]$ where L is either pyridine or a substituted pyridine have been structurally characterized. The values of Fe–N(L) are as follows: (a) $[Fe(TPP)(Py)_2]$, 2.037(1) Å, Li N, Coppens P, Landrum J. Inorg Chem 1988;27:482. (b) Ni L, Petricek V, Coppens P, Landrum J. $[Fe(TPP)(Py)_2]\cdot 2Py$, 2.039(1) Å. Acta Crystallogr, Sect C 1985;C41:902. (c) Safo MK, Nesset MJM, Walker FA, Debrunner PG, Scheidt WR. $[Fe(TMP)(4\text{-}MePy)_2]$, 2.010(2) Å; $[Fe(TMP)(4\text{-}CNPy)_2]$, 1.996(2) Å; $[Fe(TMP)(3\text{-}CNPy)_2]$, 2.026(2) Å. J Am Chem Soc 1997;119:9438.
39. Several bis-ligated iron(II) complexes of general formula $[Fe(Por)(L)_2]$ where L is either piperidine or a primary amine have been structurally characterized. The values of Fe–N(L) are as follows: (a) $[Fe(TPP)(Pip)_2]$, 2.127(3) Å, Radonovich LJ, Bloom A, Hoard JL. J Am Chem Soc 1972;94:2073. [PubMed: 4335729] (b) Munro OQ, Madlala PS, Warby RAF, Seda TB, Hearne G. $[Fe(TPP)(1\text{-}BuNH_2)_2]$ 2.039(3) Å; $[Fe(TPP)(BzNH_2)_2]$ 2.041(3) and 2.045(3) Å; $[Fe(TPP)(PhCH_2CH_2NH_2)_2]$ 2.027(2) Å. Inorg Chem 1999;38:4724. [PubMed: 11671197]The longer bond length in the piperidine

complex is rationalized in terms of steric repulsions between the piperidine hydrogen atoms and the porphyrin pyrrolic nitrogens

40. Andrew CR, George SJ, Lawson DM, Eady RR. Biochemistry 2002;41:2353. [PubMed: 11841228]
41. Denninger JW, Marletta MA. Biochim Biophys Acta 1999;1411:334. [PubMed: 10320667]
42. Négrerie M, Bouzhir L, Martin JM, Liebl U. J Biol Chem 2001;276:46815. [PubMed: 11590135]
43. Dierks EA, Hu S, Vogel KM, Yu AE, Spiro TG, Burstyn JN. J Am Chem Soc 1997;119:7316.
44. Szabo A, Perutz MF. Biochemistry 1976;15:4427. [PubMed: 184818]
45. Huheey, JE. Inorganic Chemistry. 3. Harper & Row; 1983. p. 433-435.
46. Nakamoto, K. Infrared and Raman Spectra of Inorganic and Coordination Compounds. 3. Wiley & Sons; New York: 1978. p. 279-295.
47. Vogel KM, Kozlowski PM, Zgierski MZ, Spiro TG. J Am Chem Soc 1999;121:9915.
48. Grinding of six-coordinate nitrosyl crystals in a mortar and pestle typically leads to a mixture of the desired six-coordinate species along with the five-coordinate nitrosyl as a result of loss of the neutral nitrogen ligand. Such samples judged unsatisfactory for resonance Raman measurements We now believe that will be able to prepare an adequate Raman sample, these results will be published as part of a larger study of ν(Fe–N) and ν(NO) correlations in both $\{Fe\}^6$ and $\{Fe\}^7$ species.
49. Yonetani T, Tsuneshige A, Zhou Y, Chen X. J Biol Chem 1998;273:20323. [PubMed: 9685383]
50. Nagamoto S, Nagai M, Tsuneshige A, Yonetani T, Kitagawa T. Biochemistry 1999;38:9659. [PubMed: 10423244]
51. Hayes RG, Ellison MK, Scheidt WR. Inorg Chem 2000;39:3665. [PubMed: 11196830]
52. Yoshimura T. Bull Chem Soc Jpn 1991;64:2819.
53. Yonetani T, Yamamoto H, Erman JE, Leigh JS Jr, Reed GH. J Biol Chem 1972;47:2447. [PubMed: 4336375]
54. Crystals of the diamagnetic $\{CoNO\}^8$ complex [Co(OEP)(NO)] are known to be isomorphous with [Fe(OEP)(NO)]. EPR measurements were carried out on magnetically dilute single crystals of [Co (OEP)(NO)] containing either 0.6% or 5% [Fe(OEP)(NO)].
55. Lang G, Marshall W. J Mol Biol 1966;18:385. [PubMed: 5966294]
56. Oosterhuis WT, Lang G. J Chem Phys 1969;50:4381.
57. Bohle DS, Debrunner PG, Fitzgerald J, Hansert B, Hung C-H, Thompson AJ. J Chem Soc, Chem Commun 1997:91.
58. Havlin RH, Godbout N, Salzmann R, Wojdelski M, Arnold W, Schulz CE, Oldfield E. J Am Chem Soc 1998;120:3144.
59. Champion PM, Lipscomb JD, Münck E, Debrunner P, Gunsalus IC. Biochem 1975;14:4151. [PubMed: 1182094]
60. Münck E, Groves JL, Tumolillo T, Debrunner PG. Comput Phys Commun 1973;5:225.
61. Champion, PM. Ph.D. Thesis. Univ Illinois-Urbana Champaign; 1975.

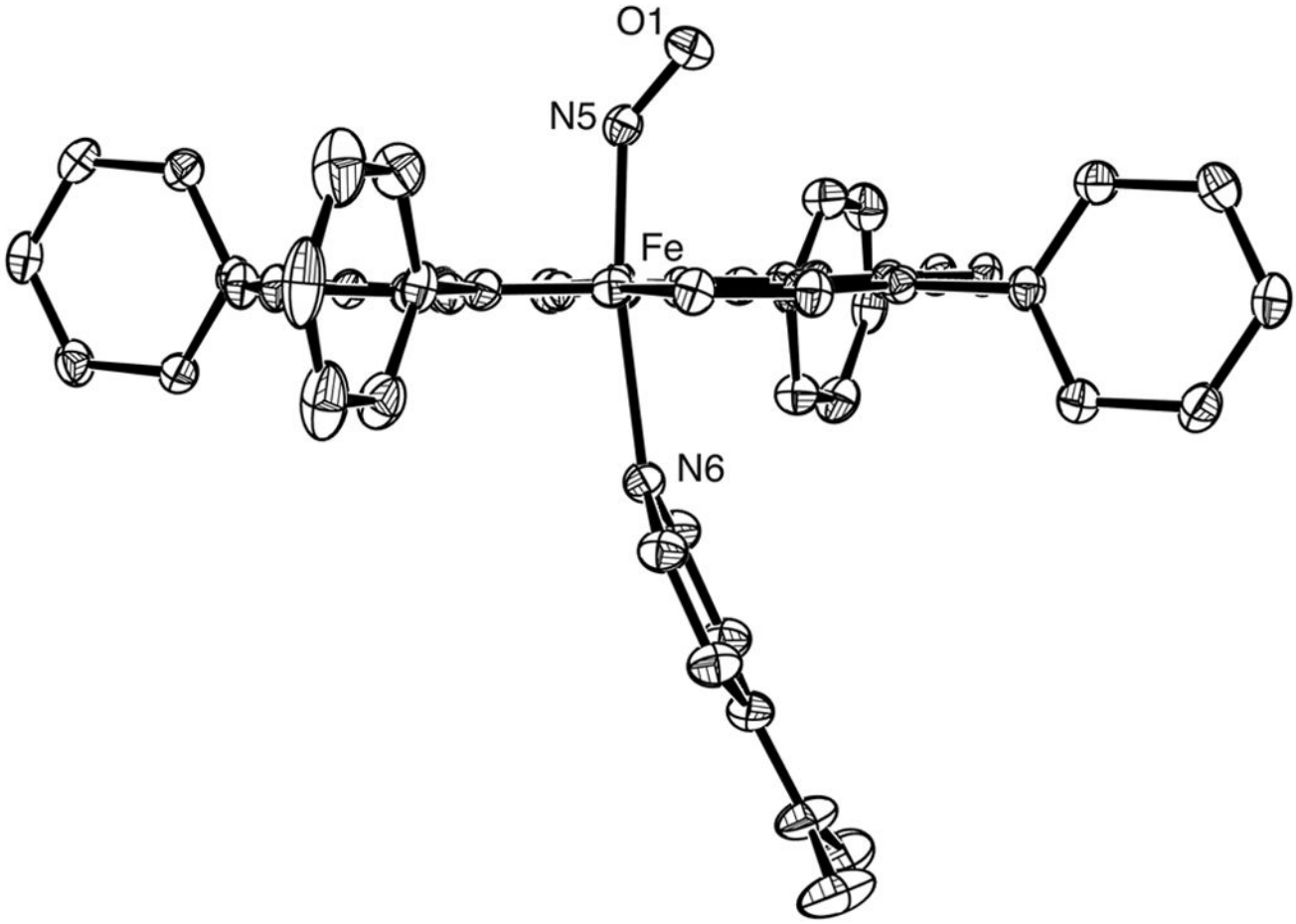

Figure 1.
ORTEP diagram of [Fe(TPP)(NO)(4-NMe_2Py)] illustrating 50% probability ellipsoids.

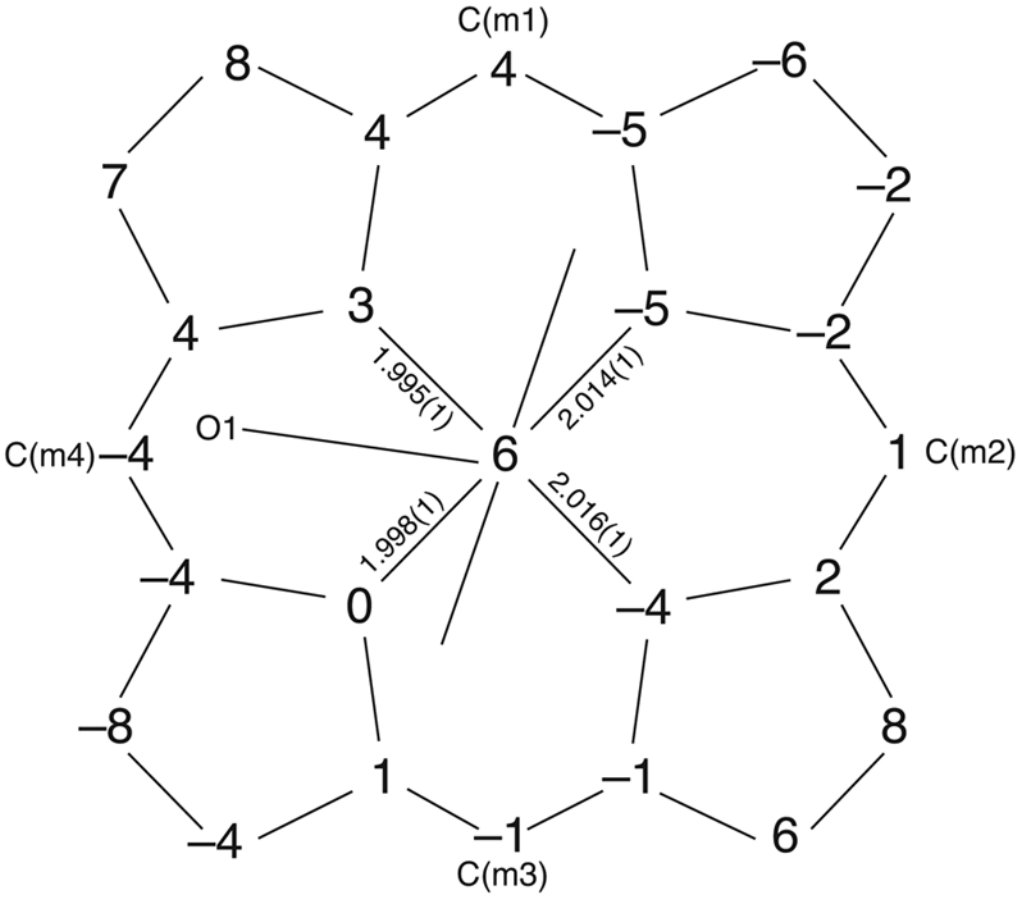

Figure 2.
Formal diagram of the porphyrinato core of [Fe(TPP)(NO)(4-NMe_2Py)] displaying the perpendicular displacements (in units of 0.01 Å) of the core atoms from the 24-atom mean porphyrin plane. Positive displacements are towards the nitrosyl coordinated face of the porphyrin. The projections of the two axial ligands are shown.

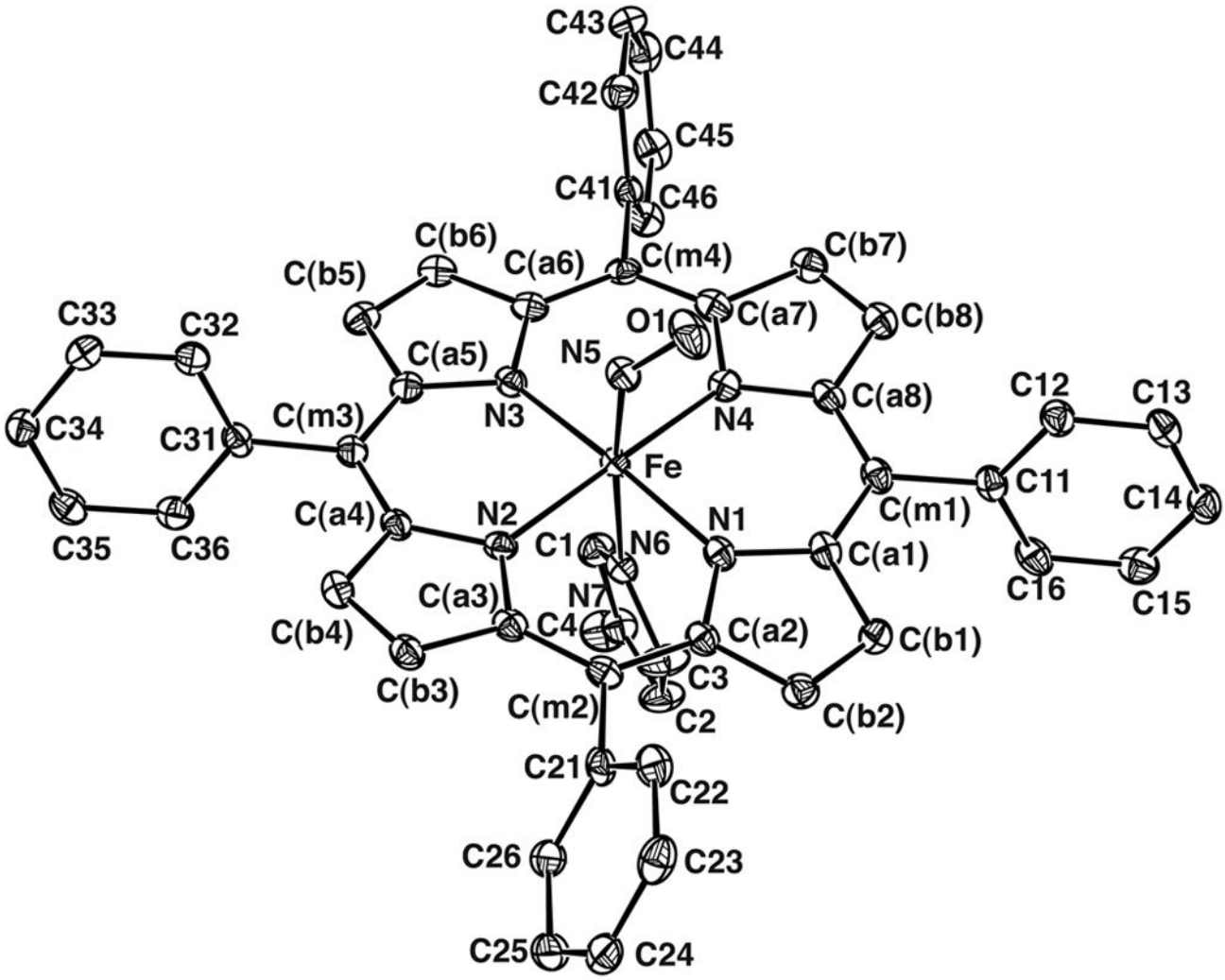

Figure 3.
ORTEP diagram of [Fe(TPP)(NO)(1-MeIm)] illustrating 50% probability ellipsoids. The labelling scheme for the porphyrin core is also shown.

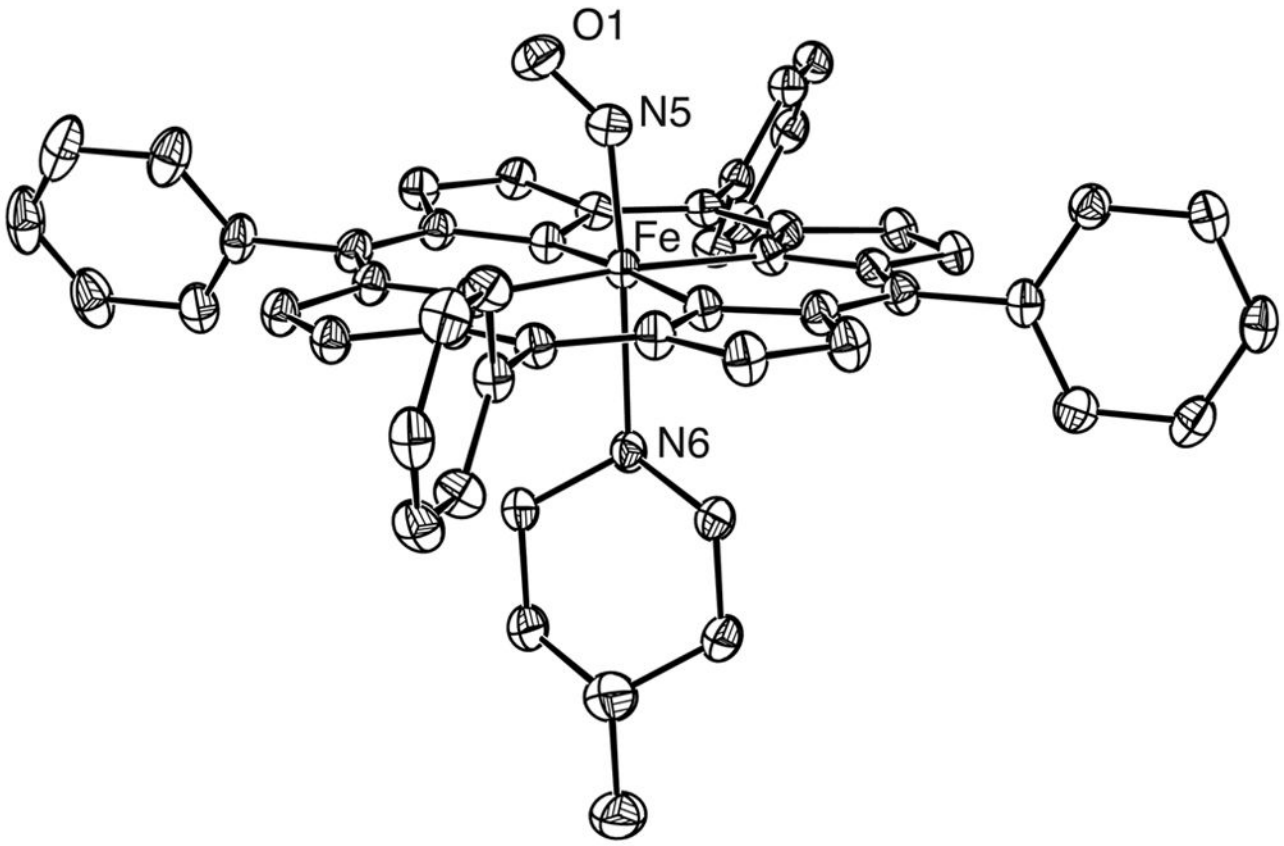

Figure 4.
ORTEP diagram of [Fe(TPP)(NO)(4-MePip)] illustrating 50% probability ellipsoids.

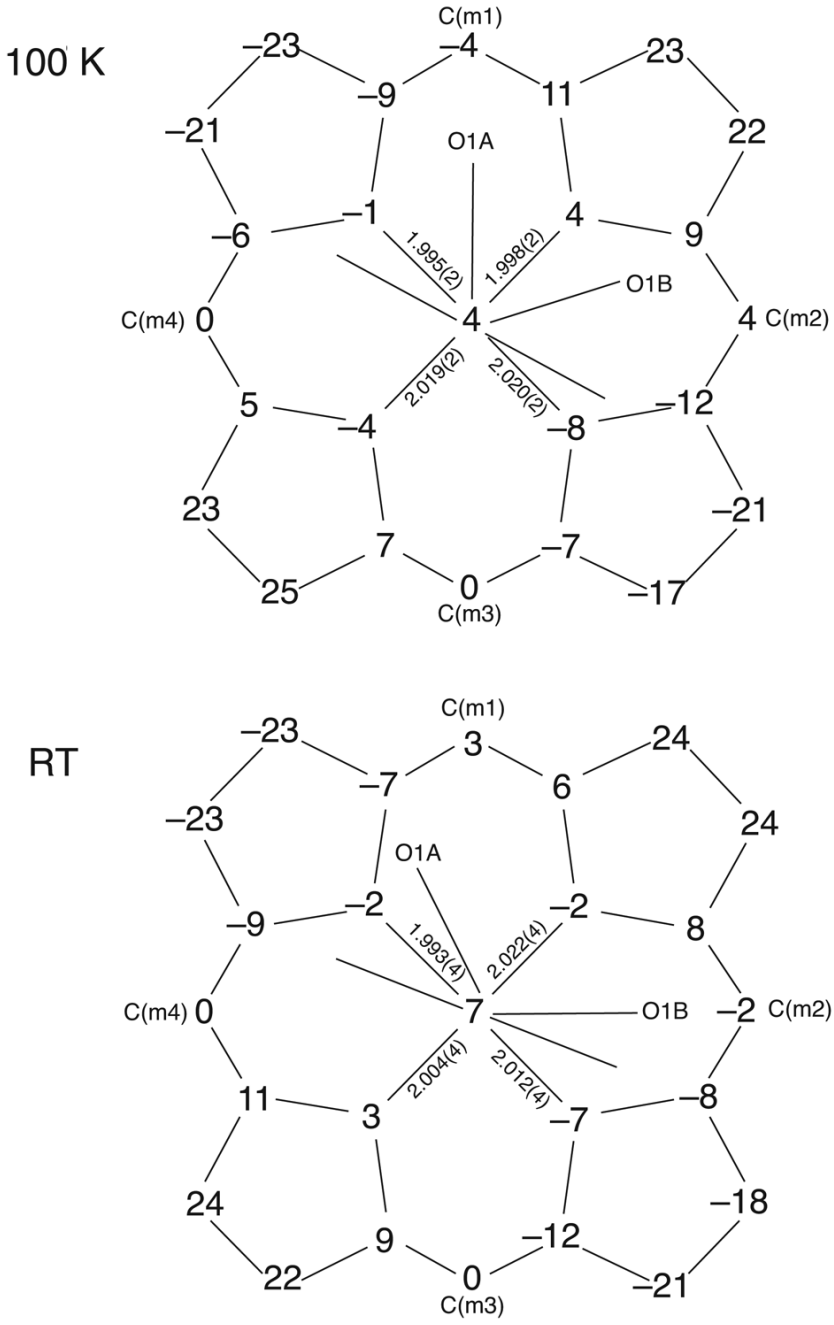

Figure 5.

Formal diagram of the porphyrinato core of [Fe(TPP)(NO)(1-MeIm)], at 100 K (top) and room-temperature (bottom), displaying the perpendicular displacements (in units of 0.01 Å) of the core atoms from the 24-atom mean porphyrin plane. Positive displacements are towards the nitrosyl coordinated face of the porphyrin. The projections of the two axial ligands are shown. The major orientation of the nitrosyl oxygen at both temperatures is denoted as O1A. Data at room temperature is taken from Reference 8.

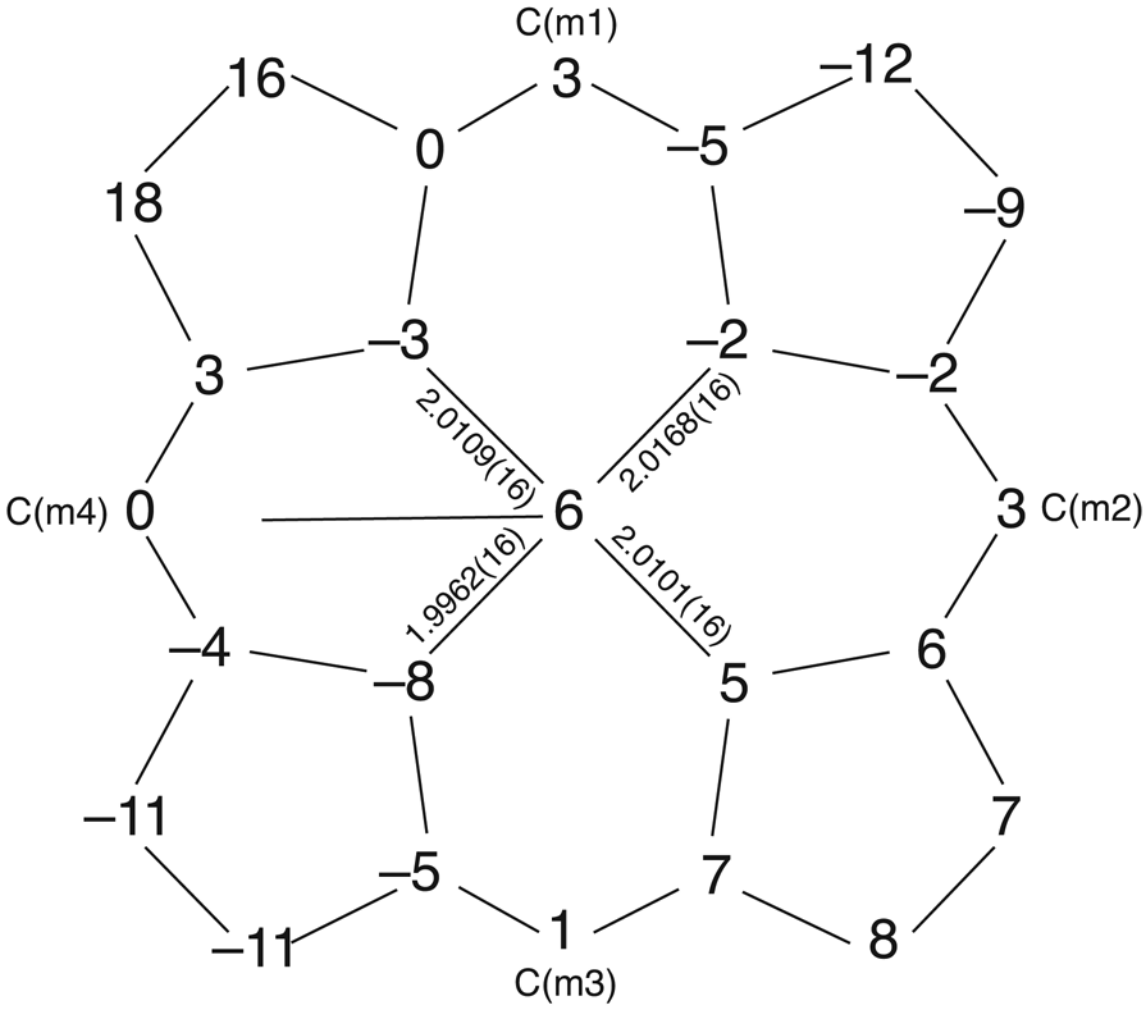

Figure 6.

Formal diagram of the porphyrinato core of [Fe(TPP)(NO)(4-MePip)] displaying the perpendicular displacements (in units of 0.01 Å) of the core atoms from the 24-atom mean porphyrin plane. Positive displacements are towards the nitrosyl coordinated face of the porphyrin. The projection of the nitrosyl ligand is shown.

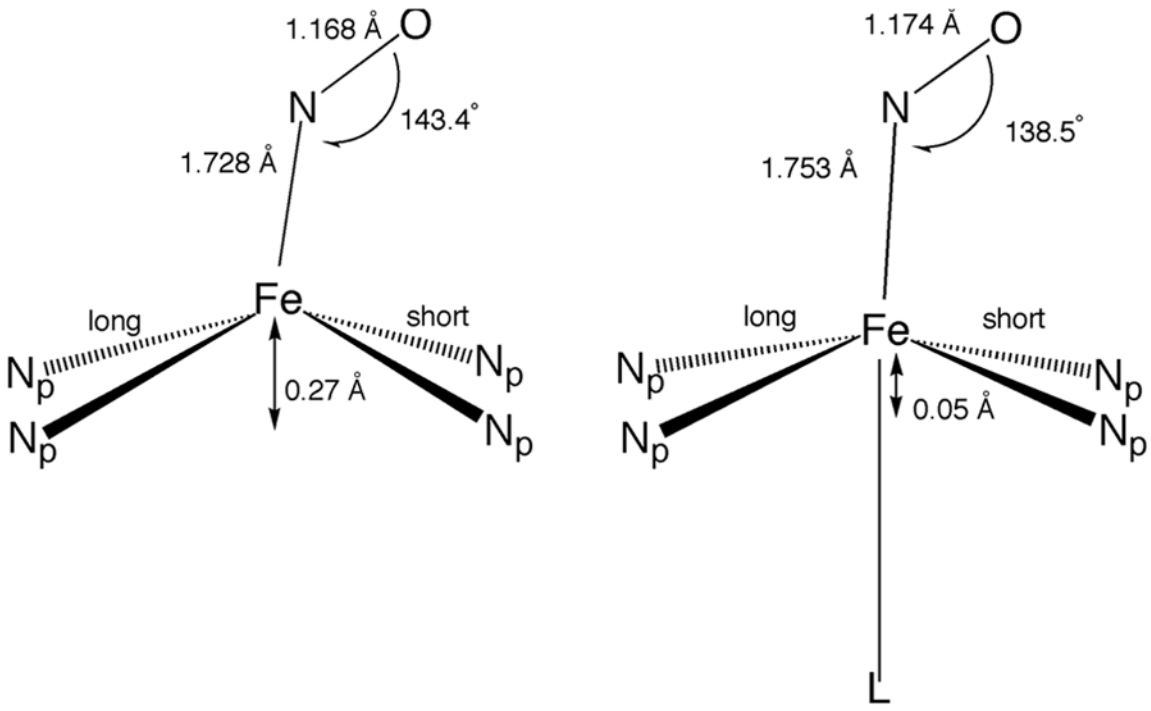

Figure 7.
Comparison of structural parameters for <[Fe(Por)(NO)]> and <[Fe(Por)(NO)(L)]>, representative geometries for the five- and six-coordinate $\{FeNO\}^7$ porphyrinate systems. Values are taken from Table 2.

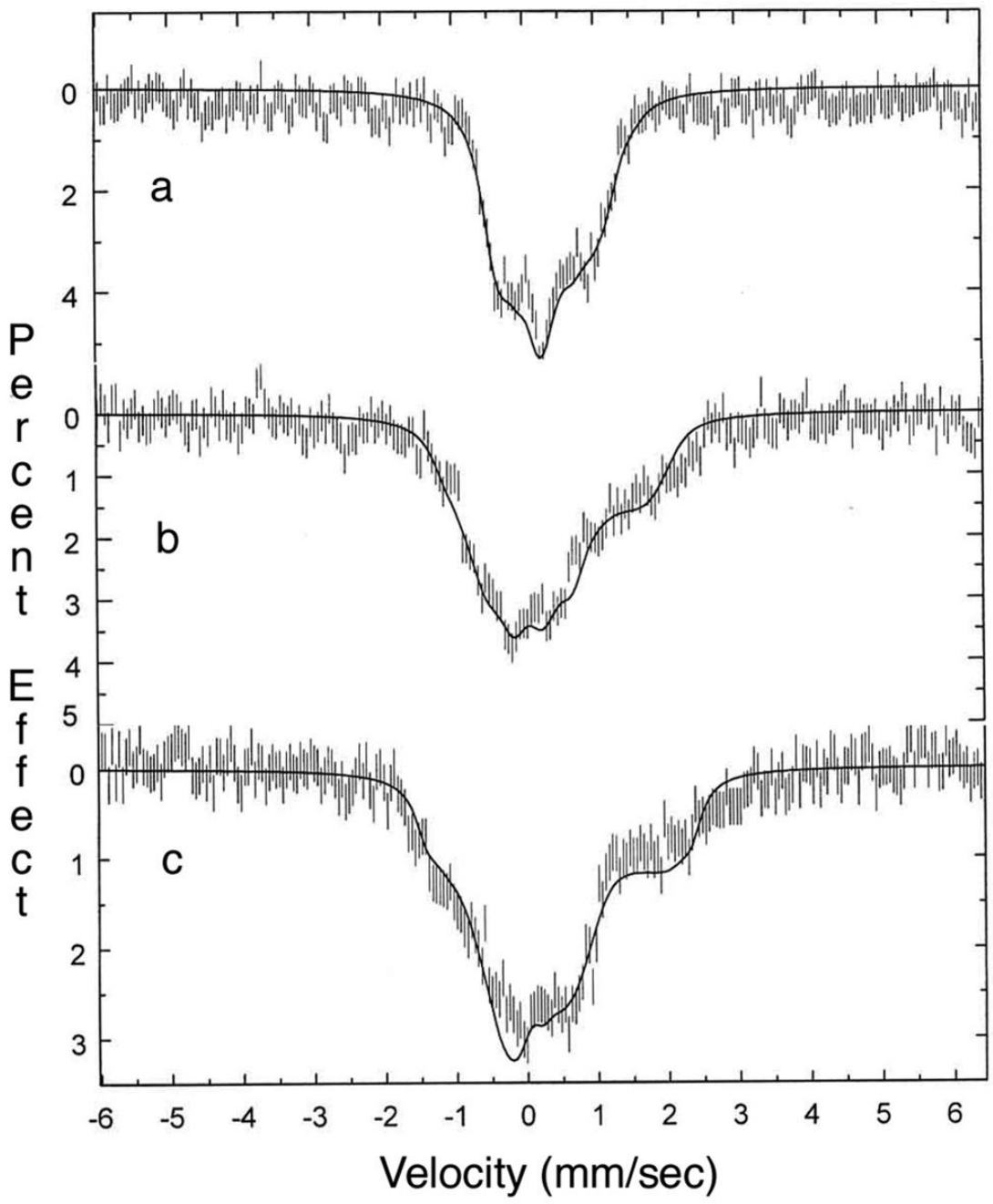

Figure 8.
Mössbauer spectra of [Fe(TPP)(NO)(1-MeIm)] at 4.2K in an applied field of a) 3 T, b) 6 T, and c) 8.8 T parallel to the γ-ray beam. The solid lines are simultaneous fits to the three spectra without rotation of the EFG tensor. The parameters determined by these fits are listed in Table 5.

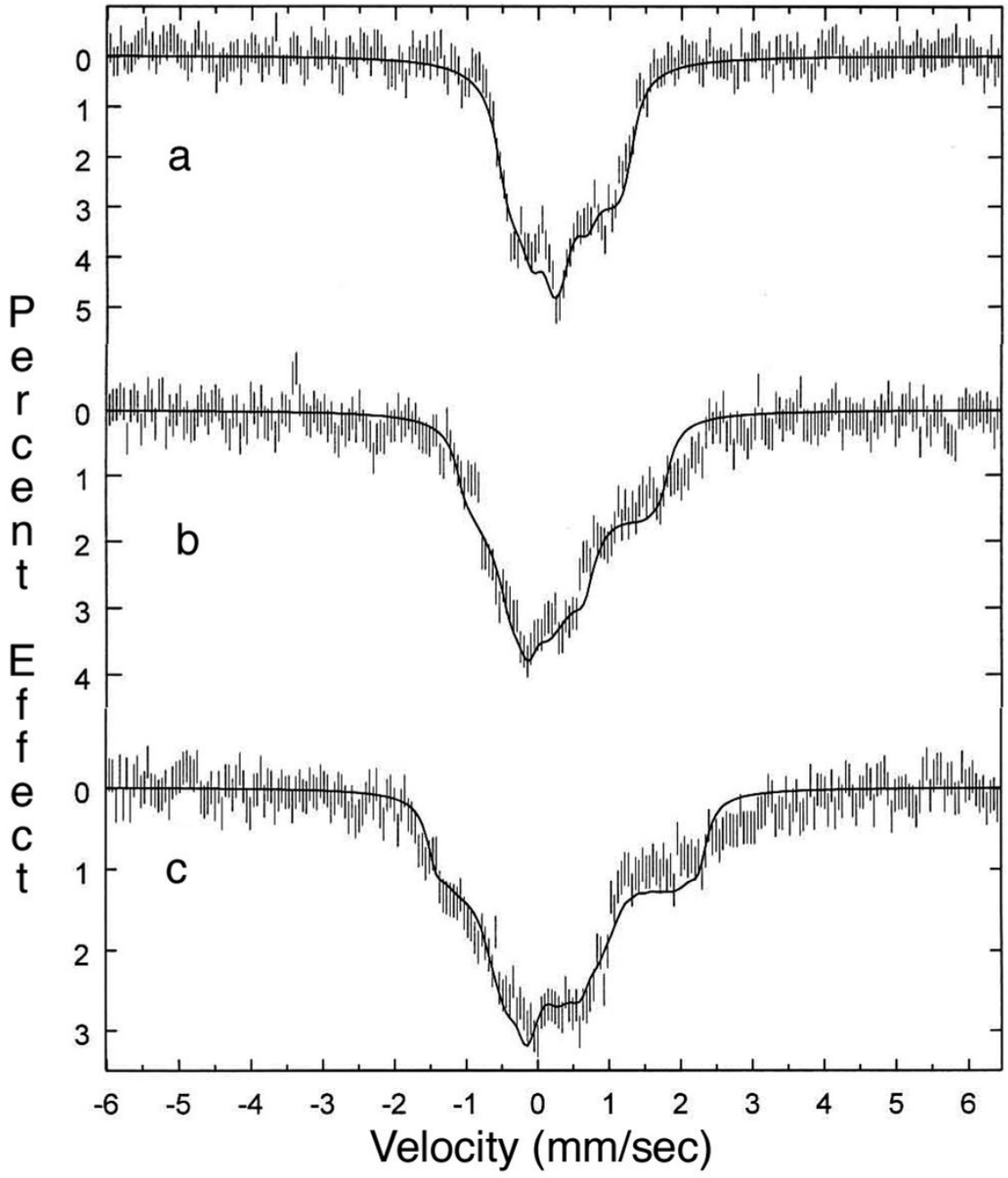

Figure 9.

Mössbauer spectra of [Fe(TPP)(NO)(1-MeIm)] at 4.2K in an applied field of a) 3 T, b) 6 T, and c) 8.8 T parallel to the γ-ray beam. The solid lines are simultaneous fits to the three spectra including Euler angles (α) and (β) to model rotation of the EFG tensor. The parameters determined by these fits are listed in Table 5.

Table 1

Complete Crystallographic Details for [Fe(TPP)(NO)(4-NMe_2Py)], [Fe(TPP)(NO)(1-MeIm)]·$CHCl_3$, [Fe(TPP)(NO)(4-MePip)]·$CHCl_3$ and [Fe(TpivPP)(NO)(Py)]·C_6H_5Cl

	[Fe(TPP)(NO)(4-NMe_2Py)]	**[Fe(TPP)(NO)(1-MeIm)]·$CHCl_3$**	**[Fe(TPP)(NO)(4-MePip)]·$CHCl_3$**	**[Fe(TpivPP)(NO)(Py)]·C_6H_5Cl**
empirical formula	$C_{51}H_{38}FeN_7O$	$C_{49}H_{35}FeN_7OCl_3$	$C_{50}H_{40}Cl_3FeN_7OCl_3$	$C_{75}H_{69}FeN_{10}O_5Cl$
FW, amu	820.73	900.04	917.09	1281.70
a, Å	10.8807(7)	17.5274(8)	17.6359(7)	18.6671(8)
b, Å	11.1420(7)	25.2009(11)	25.2877(10)	19.1581(8)
c, Å	17.1221(10)	9.6227(4)	9.9670(4)	18.4010(8)
α, deg	90.190(1)			
β, deg	93.113(1)			90.9050(10)
γ, deg	105.613(1)			
V, Å^3	1995.9(2)	4250.4(3)	4445.0(3)	6579.9(5)
space group	*P*1̄	$P2_12_12_1$	$P2_12_12_1$	*C*2/*c*
Z	2	4	4	4
crystal color	dark purple	dark purple	dark purple	dark purple
crystal dimensions, mm	0.21× 0.17 × 0.11	0.32 × 0.21 × 0.19	0.28 × 0.20 × 0.19	0.32 × 0.28 × 0.26
temp, K	100	100	100	100
total data collected	25350	46920	49041	34949
unique data	12106 (R_{int} = 0.027)	10522 (R_{int} = 0.072)	11029 (R_{int} = 0.030)	8181 (R_{int} = 0.029)
unique observed data [I > 2σ(I)]	9401	9046	10485	6430
goodness-of-fit (based on F^2)	1.031	1.070	1.046	1.771
final *R* indices	R_1 = 0.0464	R_1 = 0.0518	R_1 = 0.0411	R_1 = 0.1223
[I > 2σ(I)]	wR_2 = 0.1106	wR_2 = 0.1092	wR_2 = 0.1085	wR_2 = 0.3805
final *R* indices	R_1 = 0.0632	R_1 = 0.0637	R_1 = 0.0433	R_1 = 0.1392
(all data)	wR_2 = 0.1196	wR_2 = 0.1155	wR_2 = 0.1105	wR_2 = 0.4085

Table 2

Bonding Parameters for [Fe(Por)(NO)(L)] complexes and related species.

Complex	T (K)	Fe–N_p [a]	Fe–N (NO) [a]	∠FeNO [b]	N–O [a]	Δ, [ac]	Fe–N(L) [a]	φ(NO) [b,d]	φ(L) [b,e]	θ [b,f]	ν(NO) [g]	ref
Six-coordinate $\{FeNO\}^7$ complexes												
[Fe(TPP)(NO)(4-NMe_2Py)]	100	2.006 (11)	1.7577 (13)	139.79(12)	1.1700 (13)	0.06	2.2783 (13)	38.14	37.5	79.14	1653 [h]	tw
[Fe(TPP)(NO)(1-MeIm)]·$CHCl_3$ [i]	100	2.008 (13)	1.750(2)	137.7(2)	1.182(3)	0.04	2.173(2)	43.9	18.6	62.1	1628 [h]	tw
				137.0(8)	1.199(15)			26.9		46.5		
[Fe(TPP)(NO)(4-MePip)]·$CHCl_3$	100	2.008(8)	1.7517 (19)	138.04(17)	1.171(2)	0.06	2.2851 (19)	39.4			1642 [h]	tw
<[Fe(Por)(NO)(L)]> [j]		2.007	1.753(4)	138.5(11)	1.174(6)	0.05		40				tw
[Fe(TpivPP)(NO)(Py)]·C_6H_5Cl	100	2.009(2)	1.742(5)	133.4(5)	1.194(9)	0.21	2.260(5)	24.2	23.0	88.8	1635 [k]	tw
[Fe(TPP)(NO)(1-MeIm)]·$CHCl_3$ [i]	293	2.008 (12)	1.743(4)	142.1(6)	1.121(8)	0.07	2.180(4)	11	25.2	36	1625 [l]	8
				138.3(11)	1.144(14)			≈45		21		
[Fe(TPP)(NO)(4-MePip)]·$CHCl_3$	293	2.004(9)	1.721(10)	138.5(11)	1.141(13)	0.09	2.328 (10)	38.6			1640 [l]	10
[Fe(TPP)(NO)(4-MePip)]	293	1.998 (10)	1.740(7)	143.7(6)	1.112(9)	0.11	2.463(7)	19.6			1653-1656 [l]	10
[Fe(TpivPP)(NO)$(NO_2)]^-$ [m,n]	124	1.988(6)	1.792(8)	137.4(6)	1.176(8)	0.10	2.086(8)	41.3	44.1	85.4	1616 [l]	26
[Fe(TpivPP)(NO)$(NO_2)]^-$ [o]	127	1.986(6)	1.840(6)	137.4(6)	1.134(8)	0.09	2.060(7)	25.2	44.0	20.9	1668 [h]	26
Five-coordinate $\{FeNO\}^7$ complexes												
[Fe(OEP)(NO)] [p]	130	2.004 (15)	1.722(2)	144.4(2)	1.167(3)	0.29		37.9			1666 [h]	11
[Fe(OEP)(NO)] [q]	130	2.010 (13)	1.7307(7)	142.74(8)	1.1677 (11)	0.27		40.2			1673 [h]	11
[Fe(oxoOEC)(NO)]	130	2.009(9)	1.7320 (13)	143.11(15)	1.1696 (19)	0.26		40.9			1673 [h]	11
<[Fe(Por)(NO)]> [r]		2.008(3)	1.728(5)	143.4(9)	1.168(1)	0.27		39.6				tw
[Fe(OETAP)(NO)]	298	1.931(9)	1.721(4)	143.7(4)	1.155(5)	0.31		39.6			1666 [l]	57
[Fe(TPP)(NO)] [s]	295	2.001(3)	1.717(7)	149.2(6)	1.122(12)	0.21		40.6			1670 [l]	2

[a] Value in angstroms.

[b] Value in degrees.

[c] Displacement of the metal atom out of the 24-atom porphyrin plane towards nitrosyl group.

[d] Dihedral angle between nitrosyl and closest Fe–N_p bond.

[e] Dihedral angle between ligand plane and closest Fe–N_p bond.

[f] Dihedral angle between nitrosyl and ligand plane.

[g] Value in cm^{-1}.

[h] Nujol mull.

[i] Two positions of nitrosyl ligand observed. Values for minor position given on second line of entry.

[j] Representative values for six-coordinate $\{FeNO\}^7$ heme. Based upon data from 4-NMe_2, 4-MePip and the major nitrosyl orientation of the 1-MeIm complexes.

[k] Solution measurement in pyridine.

[l] KBr pellet.

[m] $\perp$ form.

[n] Two independent molecules, one disordered.

[o] $\parallel$ form.

[p] Monoclinic form.

[q] Triclinic form.

[r] Representative values for five-coordinate $\{FeNO\}^7$ heme. Based upon data from [Fe(oxoOEC)(NO)] and the two forms of [Fe(OEP)(NO)].

[s] Disordered molecule, 8-fold disorder of nitrosyl ligand observed.

Table 3

Details of the N_4FeNO Geometry in Five- and Six-coordinate $\{FeNO\}^7$ Porphyrinate Derivatives[a]

Complex	Fe–N(1)[b]	Fe–N(2)[b]	Fe–N(3)[b]	Fe–N(4)[b]	Δ(Fe–N_p)[b,c]	NO tilt,[d,e]	ref
			Six-coordinate $\{FeNO\}^7$ complexes				
[Fe(TPP)(NO)(4-NMe_2Py)]	**2.014(1)**	**2.016(1)**	1.998(1)	1.995(1)	0.019	2.5	tw
[Fe(TPP)(NO)(1-MeIm)]	1.998(2)	**2.020(2)**	**2.019(2)**	1.995(2)	0.023	1.8	tw
[Fe(TPP)(NO)(4-MePip)]	**2.0168(16)**	**2.0101(16)**	1.9962(16)	2.0109(16)	0.010	6.5	tw
			Five-coordinate $\{FeNO\}^7$ complexes				
[Fe(OEP)(NO)][f]	**2.016(2)**	1.989(2)	1.993(2)	**2.017(2)**	0.026	6.5	11
[Fe(OEP)(NO)][g]	**2.0226(6)**	2.0000(6)	1.9985(6)	**2.0167(6)**	0.020	8.2	11
[Fe(oxoOEC)(NO)]	2.0174(13)	**2.0141(12)**	**2.0082(13)**	1.9974(12)	—[h]	7.1	11
[Fe(OETAP)(NO)]	**1.938**	1.922	1.925	**1.941**	0.016	7.6	57

[a] Bond distance values given in bold are expected to be long, see text.

[b] Value in angstroms.

[c] Difference between average Fe–N_p(long) and Fe–N_p(short).

[d] Value in degrees.

[e] Deviation of Fe–N(NO) bond from normal to porphyrin plane.

[f] Monoclinic form.

[g] Triclinic form.

[h] Differences affected by presence of the oxopyrrole ring.

Inorg Chem. Author manuscript; available in PMC 2007 November 16.

Table 4

EPR Table

Complex	g_{max}	g_{mid}	g_{min}	a(NO)[a]	a(L)[a]	ref
[Fe(TPP)(NO)(4-NMe_2Py)][b]	2.069	2.002	1.973	23.9	7.9	tw
[Fe(TPP)(NO)(1-MeIm)][c]	2.080	2.002	1.971	22	7.2	tw
[Fe(TPP)(NO)(4-MePip)][d]	2.085	2.003	1.978	21	6.5	tw
[Fe(TPP)(NO)][b]	2.098	2.031	2.001	17.9		tw
[Fe(TPP)(NO)(1-MeIm)][e]	2.072	2.0036	1.968	22.3	7.0	52
[Fe(TPP)(NO)(Pip)][f]	2.08	2.04	2.003	21.7	5.9	3
[Fe(TPP)(NO)][f]	2.102	2.064	2.010	17.2		3
[Fe(OEP)(NO)][g]	2.110	2.040	2.012			51

[a] Value in G.

[b] CH_2Cl_2 glass at 77K.

[c] CH_2Cl_2/1-MeIm glass at 77 K.

[d] CH_2Cl_2/4-MePip glass at 77 K.

[e] Toluene glass at 77 K.

[f] Toluene glass at 120 K.

[g] Doped single crystal at 77 K.

Table 5

Mössbauer Data for [Fe(TPP)(NO)(L)] and related complexes.

Complex	Temp, K	ΔE_q[a]	δ[a]	Γ	ν	$A_{ii}/g_N\beta_N$,T	α_Q	β_Q	γ_Q	Ω[a]	χ^2[b]	ref
					Six-coordinate {FeNO}^{7} complexes							
[Fe(TPP)(NO)(1-MeIm)]	293	0.796	0.243									w
[Fe(TPP)(NO)(1-MeIm)]	150	0.75	0.31									tw
[Fe(TPP)(NO)(1-MeIm)]	50	0.75	0.33									tw
[Fe(TPP)(NO)(1-MeIm)]	4.2	0.73	0.35									tw
[Fe(TPP)(NO)(1-MeIm)].[cd]	4.2	0.73	0.34	0.39	0.92	(−14.4, −24.0, 4.2)	—	—	—	27	1.15	tw
[Fe(TPP)(NO)(1-MeIm)].[de]	4.2	0.73	0.34	0.27	0.86	(−12.5, −22.4, 4.8)	20°;	33°;	110°;	41	0.80	tw
[Fe(TPP)(NO)(4-MePip)]	293	0.94	0.26									tw
[Fe(TPP)(NO)(4-MePip)]	4.2	0.91	0.37									tw
[Fe(TPP)(NO)(4-MePip)],[cf]	4.2	0.89	0.38	0.45	0.36	(−13.5, −6.4, 9.9)	—	—	—	7.5	2.20	tw
[Fe(TPP)(NO)(4-MePip)],[ef]	4.2	0.91	0.37	0.36	0.31	(−6.1, −19.1, 12.8)	11°;	21°;	106°;	4.0	2.11	tw
					Five-coordinate {FeNO}^{7} complexes							
[Fe(TPP)(NO)]	4.2	1.24	0.35	0.42	0.32	(−25, −10.0, 13.2)	—	—	—	3.4	1.12	26
[Fe(TPP)(NO)]	4.2	1.25	0.33	0.50	0.18	(−2.5, −20.2, 13.1)	—	—	—	6.2	0.56	tw
[Fe(OEP)(NO)]	100	1.26	0.35								57	

[a] Value in mm/sec.

[b] χ^2 per degree of freedom.

[c] No EFG rotation.

[d] *c* fitted using experimental EPR *g*-values of 2.080, 2.002, 1.971.

[e] EFG rotation.

[f] fitted using experimental EPR *g*-values of 2.085, 2.003, 1.978.